

Influence of the solar atmosphere on the p -mode eigenoscillations

N.S. Dzhaliilov¹, J. Staude², and K. Arlt²

¹ Institute of Terrestrial Magnetism, Ionosphere and Radio Wave Propagation of the Russian Academy of Sciences, Troitsk City, Moscow Region, 142092, Russia (namig@izmiran.rssi.ru)

² Astrophysikalisches Institut Potsdam, Sonnenobservatorium Einsteinurm, 14473 Potsdam, Germany (jstaude, karlt@aip.de)

Received 12 April 2000 / Accepted 8 August 2000

Abstract. An asymptotic theory of global adiabatic p -modes is developed, taking into account the influence of the solar atmosphere. It is shown that waves of the whole frequency range $\nu \approx 2\text{--}10$ mHz may reach the chromosphere-corona transition region (CCTR) by means of a tunneling through the atmospheric barriers. The primary acoustic cavity inside the Sun becomes considerably extended by this way, leading to a change of frequencies: low frequencies are increased, while high frequencies are decreased. The transition from low p -mode frequencies to high peak frequencies ($\nu \gtrsim 6$ mHz) is smooth.

The locations of the turning points are determined from the wave equation for $\text{div} \cdot \vec{v}$. It is shown that the internal turning point of the acoustic cavity is strongly shifted toward the center of the Sun, while the upper turning point is shifted from the surface to CCTR. That means, the turning points cannot be located in the convective zone. A new complex integral dispersion relation for the eigenfrequencies is derived. The imaginary parts of the frequencies indicate a decay of the amplitudes, resulting from considerable energy losses by tunneling from the main cavity.

It is shown that waves with a decaying amplitude (complex frequency) may exist in a limited area only, penetration of linear p -modes to the corona is impossible. The CCTR acts as a free surface. We conclude that the p -modes may drive forced surface gravity waves at this surface.

Key words: hydrodynamics – Sun: oscillations – Sun: interior – Sun: atmosphere

1. Introduction

The p -modes are resonance oscillations of the inner acoustic cavity of the Sun formed by total reflections of waves from the inhomogeneities. The l -dependent lower boundary of the cavity arises as a result of increasing sound speed towards the center of the Sun, and waves with smaller degree l are refracted from deeper levels. The upper, almost l -independent reflecting boundary of the cavity is placed close to the surface of the Sun; it is connected with sharp gradients, especially in density (Stix 1989; Unno et al. 1989; Christensen-Dalsgaard 1994).

Send offprint requests to: J. Staude

The location of the upper boundary of the acoustic cavity for lower degrees l is determined by the condition $\omega^2 \approx \omega_c^2$ (ω is the frequency of the oscillations, ω_c is the cut-off frequency), and its dependence on ω is weak due to a sharp increase of ω_c^2 with height. As in the real solar atmosphere ω_c^2 depends on height in a complex way (see Fig. 2) potential barriers and local cavities are formed for the acoustic waves. The main photospheric barrier attains a maximum $(\omega_c^2)_{\text{max}}$ which corresponds to a critical acoustic frequency of ~ 5.5 mHz. For the low frequencies ($\nu < 5.5$ mHz) the photospheric barrier is of finite width. However, according to the generally accepted theory such low-frequency acoustic waves cannot overcome the barrier to reach the upper atmosphere. As a consequence of reflection acoustic waves become trapped in the inner cavity.

This theoretical treatment on the whole describes the observed ridge structure of the spectrum of low-frequency p -modes. Some discrepancies between observed and theoretical frequencies can be removed by changing the standard solar model (e.g., Basu et al. 1996; Morel et al. 1997; Antia & Chitre 1998). However, some recent observations from SOHO suggest to correct some features of the p -modes theory as well as to consider the influence of the atmosphere on the spectrum of p -modes in more detail. Let us discuss some of these aspects.

1.1. High frequency p -modes

Similarly to the behavior of a quantum-mechanical system a discrete spectrum of the p -modes is formed for the frequencies $\nu < 5.5$ mHz (the maximum of the potential barrier) and this spectrum is continuous beyond this maximum, for $\nu > 5.5$ mHz. However, this theoretical prediction is not confirmed by numerous observations of velocity and intensity fluctuations. Instead, a high-frequency (up to 12 mHz) ridge structure in the spectrum of p -modes is detected (Libbrecht 1988; Duvall et al. 1991; Fernandes et al. 1992; Kneer & von Uexküll 1993; Garcia et al. 1998; Antia & Basu 1999). The obvious question arises why the peaks are formed above the acoustic cut-off frequency of 5.5 mHz, where the waves are able to propagate in the atmosphere and thus should not be trapped in a cavity below the photosphere.

Kumar & Lu (1991) have suggested that the peaks at high frequencies are formed as a result of interference between waves

returning from inside and those traveling from the acoustic source. The peak frequencies in this case are strongly dependent on the assumed spatial position of the source. It should be noted that all resonant frequencies are the result of an interference of traveling waves. However, why the mechanism of Kumar & Lu (1991) would work for the high frequencies only, but not for the whole range 1.5–12 mHz of p -modes? In our opinion a more realistic idea has been suggested by Balmforth & Gough (1990): they have considered the high-frequency peaks as the result of reflections of waves from the transition layer CCTR, where the temperature rises by a factor of 100 over a distance much smaller than the wavelength. Gabriel (1992) has shown that the surface boundary conditions such as running waves in the corona and perfect reflection at the bottom of the corona exert an influence on a p -mode spectrum. To find model-independent characteristics of the spectrum he has replaced the real atmospheric wave potential by stepwise constant pieces.

The high-frequency modes appear as a continuous extension of the low-frequency p -modes in the diagnostic $(\nu - l)$ diagram and extend up to frequencies of at least 12 mHz (e.g., Libbrecht 1988; Duvall et al. 1991; Elsworth et al. 1993). Both the peak frequencies in the high-frequency spectrum and the p -modes at low frequencies obey the *same* dispersion relation (Duvall's law) which is derived for the p -mode acoustic cavity.

If low-frequency waves are really turning back totally from the lower boundary of the photospheric barrier and if for high-frequency waves this turning point is abruptly shifted up to CCTR, a sharp change in the ridge structure around 5.5 mHz must be observed. Such a conclusion can be drawn as the eigenfrequencies are very sensitive to any shift of the turning points. However, such a sharp shift of the turning point up to about 2000 km is not present in the observed spectrum of the p -modes.

1.2. The chromospheric modes

The next established fact derived from observations is absence of eigenmodes of the chromospheric cavity in the power spectrum. These modes should manifest themselves as horizontal bright streaks in the frequency range $\nu < 5.5$ mHz (Duvall et al. 1991; Fernandes et al. 1992; Kneer & von Uexküll 1993; von Uexküll & Kneer 1995; Al et al. 1998). Variations of intensity and of the profiles of 19 ultraviolet lines have been observed by SOHO/SUMER, but no evidence of the existence of the chromospheric modes was found (Gouttebroze et al. 1999).

The chromospheric cavity is located between the photospheric barrier and CCTR (see Fig. 2). If the photospheric barrier and CCTR would be ideal reflectors, then the eigenfrequencies of the chromospheric cavity should be located in the range $2 \lesssim \nu \lesssim 6$ mHz. However, due to the limited widths of the photospheric barrier and of the chromospheric cavity only the first two modes could be excited (McKenzie 1971). These modes correspond to the upper part of the potential barrier, where its width is narrow enough (comparable to or less than the wavelength). That means, it becomes doubtful whether the waves moving downward from CCTR are reflected from the barrier and become trapped. Deubner & Fleck (1990) suppose that the

small-scale inhomogeneities in the chromosphere and the structure of the upper boundary will prevent the development of these modes. Gabriel (1992) showed that the strong damping of these modes will obstruct any attempt to observe these modes.

The numerical calculations by Ando & Osaki (1977) and Ulrich & Rhodes (1977) with an upper boundary condition at CCTR have shown some l -independent crossings of the ridge branches in the $(\nu - l)$ diagram. These over-crossings have been interpreted as the appearance of the first eigenmode of the chromospheric cavity at 4.13 mHz. Similar numerical calculations have been done by Antia & Basu (1999) for the case of the $(\nu - l)$ ridges which continue up to 10 mHz. They got a series of such avoided crossings between the p -mode ridges. Similar crossings are seen even at 10 mHz. Hence such l -independent crossings are not the trace of chromospheric modes. These crossings appeared only when the upper atmosphere was included into the consideration of the waves. In this case the calculated frequencies appeared worse in comparison to those for which the atmospheric influence was neglected. That means, the problem with the upper boundary condition is obvious.

Antia & Basu (1999) have calculated the separation $(\nu_{n+1,l} - \nu_{n,l})$ of the observed frequencies between adjacent modes. In the domain of the frequencies 5.5–6.0 mHz these separations show some remarkable deviations from the normal behavior. We think these deviations are caused by the abrupt end of the photospheric barrier due to the atmospheric structure.

Some other observational facts concerning the low-frequency p -modes require a theoretical treatment too. The information about the atmospheric behavior of waves is mainly extracted from $(V - V)$ and $(I - I)$ phase spectra. The results are somewhat inconsistent, but on the whole the observed waves are either standing or progressive, depending on the heights where the lines are formed and on the frequency of the observed oscillations (see, e.g., Fleck & Deubner 1989, Muglach & Fleck 1999). The p -modes are detected at almost all levels of the atmosphere. For example, upward propagating waves have been observed in the photosphere by Staiger (1987) and by Fleck & Deubner (1989). The propagating behavior of 5-min oscillations has been detected in the upper atmosphere and CCTR (Baudin et al. 1996; Steffens & Deubner 1999). Power spectra for the intensities of several lines formed in the upper transition region in the 2–5 mHz range with the largest power peak at 3 mHz were observed by Doyle et al. (1998).

Another problem is why for the high- l f -modes we have $\omega^2 \neq gk_{\perp}$. The deviation from the classical dispersion relation could be due to the influence of a random flow (see Murawski 2000 a, b; Medrek & Murawski 2000, and the references given there).

The problems mentioned above prompted the idea that the formation of the whole range (2–10 mHz) of observed frequencies of the oscillation modes is based on the same mechanism. Obviously transmission of low-frequency ($\nu < 5.5$ mHz) p -modes through the photospheric barrier is significant. Waves partially passing through the barrier and reaching CCTR extend the width of the main cavity which should lead to a decrease of the eigenfrequencies. Thus, there arises the possibility to get the

observed frequencies of p -modes without changing the standard solar model. Some authors tried to explain the frequency discrepancy between theory and observations by the influence of turbulent convection (Rosenthal et al. 1999, Böhmer & Rüdiger 1999, Gabriel 2000).

In the present work we develop an asymptotic theory of adiabatic p -modes in order to clarify the role of the solar atmosphere in the formation of resonant frequencies. The asymptotic formula for the eigenfrequencies has first been derived by Vandrakurov (1967) and further extended by Tassoul (1980). Due to the frequency discrepancy problem the asymptotic theory of p -modes has been further developed, e.g., by Tassoul (1990), Roxburgh & Vorontsov (1994), and Willems et al. (1997). In these papers a second-order asymptotic theory for the adiabatic oscillations of low-degree p -modes avoiding the Cowling approximation has been considered. The influences of the local effects of gravity and of buoyancy forces on the acoustic waves in the solar core (the curvature effects) have been taken into account. As a result, the time needed for an acoustic wave to propagate from the center is increased, and the inner boundary of the acoustic cavity is displaced slightly towards the center. Thus, the frequencies of p -modes are decreased. However, for the normal solar model the second asymptotic approximations of the eigenfrequencies do not lead to satisfying results. In the authors opinion this is caused by the influence of the surface layers of the Sun.

It has already been mentioned that the complexity introduced by the consideration of the atmosphere in the analytic theory of p -modes is caused by the appearance of several cavities and barriers with different thicknesses. As a result of the tunneling the waves should reach CCTR. The phenomenon of wave tunneling has already been studied by Lamb (1908). The p -mode energy leakage into the corona has been considered by e.g. Ando & Osaki (1977), Ulrich & Rhodes (1977), Balmforth & Gough (1990), and Milford et al. (1993). The dependence of p -mode frequencies on the atmospheric temperature has been investigated in several papers, e.g. by Evans & Roberts (1990), Hindman & Zweibel (1994), Christensen-Dalsgaard & Thompson (1997), and Steffens & Schmitz (2000). Most of these authors assumed analytic temperature profiles for a polytropic, isothermal and plane-parallel atmosphere. This assumption seems to be justified for high-degree f - and p -modes.

In the present work the eigenvalue problem is solved for a realistic model of the solar interior and atmosphere with all possible kinds of turning points. In Sect. 2 we will discuss basic features of the problem using a simplified model of isothermal layers, where the role of wave tunneling in the frequency shifts is shown. The main equation for the adiabatic spherical p -modes in the Cowling approximation, including the curvature effects, is derived in Sect. 3. In Sect. 4 the new locations of the turning points are discussed, when the tunneling of waves through atmospheric barriers is taken into account. For high harmonics the asymptotic solutions are derived (Sect. 5 and Appendix), and using these solutions the eigenvalue problem is considered. The integral dispersion relations for the complex eigenfrequencies of radial and non-radial oscillations are derived in Sect. 6. In

Sect. 7 a table of the calculated frequencies of radial waves and a comparison with the observed frequencies are presented. Finally, in Sect. 8 we discuss the possibilities for a further development of the theory of p -modes and of the upper boundary condition.

2. Isothermal layers model

Using a simple model with isothermal layers (temperature $T = \text{const.}$), we will investigate in this section what we can expect when the tunneling of waves through the acoustic barrier is taken into account. Fig. 2 shows that in a realistic model of the solar atmosphere we have a variety of cavity-tunnel structures. Simplifying the situation, let us consider an atmosphere consisting of three isothermal layers with different temperatures T_1 , T_2 , and T_3 , where the middle layer is cooler than the upper and lower layers, $T_2 < T_{1,3}$. The corresponding constant sound speeds obey the same relation: $c_2 < c_{1,3}$. This case is chosen to mimic the solar atmosphere with a temperature minimum region. The ratio T_3/T_1 in the real atmosphere could be smaller or larger than one. We use a Cartesian coordinate system, with the origin of the z -axis at the boundary between the first and the second layer. The z -axis is pointed upwards against the gravity $g = \text{const.}$ The width of the middle layer is finite and is denoted by z_t . Then, for small-amplitude adiabatic perturbations in isothermal, plane-parallel layers the vertical velocity V_z is given by Stix (1989):

$$V_z \sim \exp \left[-i\omega t + \left(\frac{1}{2H} \pm ik_z \right) z \right], \quad (1)$$

where ω is the angular frequency, H is the pressure scale-height, and k_z is the vertical wave number,

$$k_z^2 = \frac{\omega^2 - \omega_c^2}{c^2} + k_\perp^2 \left(\frac{N^2}{\omega^2} - 1 \right), \quad (2)$$

$$H = \frac{c^2}{\Gamma_1 g}, \quad \omega_c = \frac{c}{2H} = \frac{\Gamma_1 g}{2c}, \quad N = (\Gamma_1 - 1)^{1/2} \frac{g}{c}.$$

Here ω_c is the acoustic cut-off frequency, c is the adiabatic sound speed, N is the Brunt-Väisälä frequency, Γ_1 is the adiabatic exponent, $g = 0,274 \text{ km/s}^2$, $k_\perp^2 = l(l+1)/R_\odot^2$ is the squared horizontal wave number, and l is the spherical harmonic degree.

In the isothermal layers model c_2 corresponds to the sound speed at the temperature minimum. For c_1 it is chosen the value of the sound speed at the level from which the waves are reflected for a given frequency. So the condition $\max(\omega_{c_1}^2, \omega_{c_3}^2) \leq \omega^2 \leq \omega_{c_2}^2$ is supposed to be satisfied. Here $\omega_{c_1}^2$, $\omega_{c_2}^2$, and $\omega_{c_3}^2$ are the squared cut-off frequencies in the corresponding layers, for which $\omega_{c_2} > \omega_{c_{1,3}}$ are fulfilled. Hence for low l in the lower and upper layers $k_z^2 > 0$ (oscillatory behavior), and in the middle layer $k_z^2 < 0$ (evanescent behavior). As a consequence of that an evanescent zone (tunnel) is settled between two propagation zones, where the wave amplitudes are exponential functions of z . Let us assume $k_1^2 = k_z^2|_{c=c_1}$, $k_2^2 = -k_z^2|_{c=c_2}$, and $k_3^2 = k_z^2|_{c=c_3}$. Here $k_{1,2,3}^2 \geq 0$. Then, the solutions in the three layers can be written in the form:

$$V_{z_1} = (C_1 e^{ik_1 z} + C_2 e^{-ik_1 z}) e^{z/2H_1}, \quad z \leq 0, \quad (3)$$

$$V_{z_2} = (D_1 e^{k_2 z} + D_2 e^{-k_2 z}) e^{z/2H_2}, \quad 0 \leq z \leq z_t, \quad (4)$$

$$V_{z_3} = M e^{(ik_3 + 1/2H_3)z}, \quad z \geq z_t. \quad (5)$$

Here C_1, C_2, D_1, D_2 , and M are arbitrary constants which can be determined by the boundary conditions. Our task is to consider the waves incident from the first layer to the evanescent layer, the reflection, and the tunneling of them to the upper layer. In the case of infinitely broad tunnels ($z_t \rightarrow \infty$) we must assume $D_1 = 0$ to satisfy the regularity of the solution. This case is the same as that in the usual asymptotic theory of p -modes without taking into account of presence of the atmosphere. In this case the waves are totally reflected from the evanescent zone. Of course, in this case for the real Sun Eq. (3) is replaced by a more exact solution. Here a finite tunnel ($z_t < \infty$) will be considered.

First, let us consider free (not trapped) oscillations in the first layer. To find the reflection coefficient $R = C_2/C_1$ we have to compare the amplitudes of incident and reflecting waves (C_1 and C_2) with the amplitudes of the outgoing wave (M) in the upper layer. For this purpose we use the continuity condition for the flux of mass and for pressure at the interfaces ($z = 0$ and $z = z_t$): $\{\rho V_z\} = 0$ and $\{p\} = 0$. Here $\{a\}$ denotes the difference of the variable a at the interfaces. For linear waves these conditions are reduced to $\{\rho_0 V_z\} = 0$ and $\{\frac{dV_z}{dz}\} = 0$. Matching solutions (3)–(5) at the interfaces, we have the relations

$$R = \frac{C_2}{C_1} = \frac{w + D_1/D_2}{1 + wD_1/D_2}, \quad \frac{D_1}{D_2} = \frac{1 + ia}{1 - ia} e^{-2k_2 z_t}, \quad (6)$$

$$w = -\frac{1 + ib}{1 - ib}, \quad a = \frac{T_3 k_3}{T_2 k_2}, \quad b = \frac{T_1 k_1}{T_2 k_2}.$$

For a wide tunnel $k_2 z_t \gg 1$ we get $R \approx w$ and hence the reflection is total, $|R| = 1$. However, for a narrow tunnel $|R| < 1$. In the particular case of $T_1 = T_3$ we have $a = b$. Then, from Eq. (6) we get

$$|R|^2 = 1 - \frac{4a^2}{(1 + a^2)^2 \sinh^2(k_2 z_t) + 4a^2}. \quad (7)$$

In the limit $k_2 z_t \rightarrow 0$, $|R| \rightarrow 0$, and if $k_2 z_t \gg 1$ we have $|R| \rightarrow 1$. That means, a part of the energy of the incident waves is tunneled to the upper layer. For frequencies $\omega \lesssim \omega_{c_2}$ when $k_2 \rightarrow 0$ a considerable amount of energy is tunneled even if the tunnel is wide.

Now let us consider the case when the waves are trapped in the bottom layer. In the case of nonradial waves there exists an inner turning point $z = -r_t(\omega, l)$ below which the amplitudes of waves tend to zero. For the radial oscillations this point is the center of the Sun, $r_t = R_\odot$. Using the condition $V_{z_1} = 0$ at $z = -r_t$, we get from Eq. (3)

$$R = \frac{C_2}{C_1} = -e^{-2ik_1 r_t}. \quad (8)$$

For real frequencies this means a condition of total reflection of waves from the inner levels, $|R| = 1$. For the eigenfunctions we have

$$V_{z_1} = C \frac{\sin[k_1(z + r_t)]}{\sin(k_1 r_t)} e^{z/2H_1}, \quad (9)$$

where $C = \text{const}$. Hence, we see that the last node is located at the turning point $z = -r_t$, and at the interface ($z = 0$) the waves have a maximum amplitude. From Eqs. (6) and (8) we derive the transmission condition

$$F(\omega) = f(\omega) - (1 + ia) \frac{1 - \tanh(k_2 z_t)}{1 - ia \tanh(k_2 z_t)} = 0, \quad (10)$$

$$f(\omega) = 1 + b \cot(k_1 r_t). \quad (11)$$

The condition Eq. (10) has complex roots only if the width of the tunnel is finite: $\omega = \omega_1 - i\omega_2$ with $\omega_2 > 0$. The real part of the frequency depends on the cavity structure; it is defined by the width and the equilibrium model of the cavity. Similarly, the imaginary part ω_2 is a consequence of wave tunneling. We can choose ω_2 for the eigenvalues of ω_1 such that the condition $|R| \ll 1$ in Eq. (6) is satisfied. That means that even for a wide tunnel $|2k_2 z_t| \gg 1$ we can expect a stronger transmission of wave energy through the tunnel.

As already mentioned the role of the atmosphere is excluded in the standard asymptotic theory by assuming total reflection from the barrier which corresponds to $z_t \rightarrow \infty$. In this case $D_1 = 0$ in Eq. (4). Then, from Eq. (10) we obtain

$$f(\omega; l) = 0. \quad (12)$$

A root of this equation is denoted by ω_0 to distinguish them from the common root ω when $z_t \neq \infty$. For the real Sun the lower isothermal layer is replaced by the internal solar model, and the function $f(\omega)$ in Eq. (11) is replaced by

$$f(\omega_0) = \int_{r_t}^{R_\odot} k_z(\omega_0, l; r) dr - \pi \left(n + \frac{1}{2} \right), \quad (13)$$

where $n = 1, 2, \dots$ are the orders of the spherical harmonics and $r = R_\odot + z$. A detailed study of Eq. (10) is not necessary as the isothermal layers model is a very crude approximation for the solar atmosphere. Based on Eqs. (10) and (13) it may be shown how the eigenfrequencies change when the tunneling of waves is included. It is clear that the frequencies will be altered only slightly. So, we can define $\omega = \omega_0 + \delta\omega$, where ω_0 is a root of Eq. (12) without tunneling, and $|\omega_0| \gg |\delta\omega|$. From the Taylor expansion of $F(\omega_0 + \delta\omega)$ we have

$$\delta\omega \approx -\frac{F(\omega_0)}{\frac{\partial F}{\partial \omega}|_{\omega=\omega_0}}. \quad (14)$$

Using the simplifying condition $\text{Re}(k_2 z_t) \gg 1$ we have

$$\delta\omega \approx \frac{1 + ia}{1 - ia} [1 - \tanh(k_2 z_t)] \frac{1}{\partial f / \partial \omega}, \quad (15)$$

$$\frac{\partial F}{\partial \omega} \approx \frac{\partial f}{\partial \omega}|_{\omega_0} \approx \omega_0 \int_{r_t}^{R_\odot} \frac{1 - S_l^2 N^2 / \omega_0^4}{c^2 k_z} dr > 0. \quad (16)$$

S_l is the Lamb frequency. Here we are interested in the function $\text{Re}(\delta\omega(\omega_0))$ only. It is defined by

$$\text{Re}(\delta\omega) \sim 1 - a^2 = 1 - \frac{T_3 \omega_0^2 - \omega_{c_3}^2}{T_2 \omega_{c_2}^2 - \omega_0^2}, \quad (17)$$

where $\omega_{c_3}^2 < \omega_0^2 < \omega_{c_2}^2$. It follows that for low frequencies of the p -modes, $\omega_0 \rightarrow \omega_{c_3}$, we have $\text{Re}(\delta\omega) > 0$ and hence

$\omega > \omega_0$. This means that the effect of tunneling is to increase low frequencies. As a consequence of that we expect a difference $\Delta = (\omega_{\text{obs}} - \omega) < 0$, where ω_{obs} is the observed p -mode frequency. For high frequencies $\omega_0 \rightarrow \omega_{c_2}$ and we have $\text{Re}(\delta\omega) < 0$ and $\omega < \omega_0$. This means that the effect of tunneling is to decrease high frequencies, and $\Delta > 0$. As it is expected, this effect grows with frequency.

For the frequency $\omega^2 = \omega_{c_2}^2 T_2 / (T_2 + T_3)$ $\text{Re}(\delta\omega) = 0$. For the temperature minimum region $T_2 = 4170$ K, $c_2 = 6.7$ km/s, and $\omega_{c_2} = 3.4 \times 10^{-2}$ s $^{-1}$. If we take $T_3/T_2 = 4.78$ (beginning of the temperature plateau at the base of CCTR), we have $\text{Re}(\delta\omega) = 0$ for the frequency $\omega = 2 \times 10^{-2}$ s $^{-1}$ ($\nu = 3.3$ mHz).

In this section we have shown, on the basis of a simple isothermal layers model, that taking an influence of the atmosphere on the p -modes into account has a great chance to solve the frequency discrepancy problem. According to such an approach low frequencies are increased while high frequencies are decreased. A crossover ($\Delta \approx 0$) occurs at $\nu \approx 3.3$ mHz. The subsequent sections are devoted to a more accurate calculation of the frequency change $\delta\omega$ for a real solar atmosphere model.

3. Basic equations

We use the equations of hydrodynamics which describe the oscillations of a star in the case of a non-magnetic, self-gravitating system; we consider linear, adiabatic waves in a non-rotating, convective-free system in the Cowling approximation. The Eulerian perturbation is denoted by a prime, while the Lagrangian perturbation is denoted by a symbol δ . We write

$$U(r, \vartheta, \varphi) = \nabla \cdot \vec{\xi} = -\frac{\delta\rho}{\rho} = -\frac{1}{\Gamma_1} \frac{\delta p}{p}, \quad (18)$$

where ρ denotes the density, p the pressure, and the fluid velocity is written as $\vec{v} = \frac{\partial \vec{\xi}}{\partial t}$. $\vec{\xi} = (\xi_r, \xi_\vartheta, \xi_\varphi)$ is the displacement vector.

For the basic equations a separation of all variables into radial and angular parts in spherical harmonics is possible in the form

$$p'(t, r, \vartheta, \varphi) = p'(r) Y_l^m(\vartheta, \varphi) e^{-i\omega t}, \quad (19)$$

where $l = 0, 1, 2, \dots$ is the degree of the spherical surface harmonics and $m = 0, \pm 1, \dots, \pm l$ is the azimuthal order of the harmonics. Here we use the same symbols to denote the radial parts of the variables. Working out the equations, we obtain a set of ordinary differential equations as follows:

$$\begin{aligned} \rho g \xi_r - \rho c^2 U &= p', \\ -\omega^2 \xi_r + \frac{1}{\rho} \frac{dp'}{dr} + g \left(\frac{\xi_r}{H} - U \right) &= 0, \\ r^2 \left(\omega^2 + 4\pi G \rho + g \frac{d}{dr} \right) \rho \left(\frac{\xi_r}{H} - U \right) + \\ + \frac{d}{dr} \left(r^2 \frac{dp'}{dr} \right) - l(l+1)p' &= 0. \end{aligned} \quad (20)$$

Here the gravitational acceleration satisfies the Poisson equation: $dg/dr = 4\pi G \rho - 2g/r$, where G is the gravitational constant, $1/H = -d \ln \rho / dr$ is the inverse density scale height, and $c^2 = \Gamma p / \rho$ is the squared sound speed.

We want to construct an equation of second order in $U(r)$, which is free from an internal singularity for smaller l . From Eq. (20) the variable $p'(r)$ can be eliminated to get

$$\xi_r = -\frac{g\omega^2 r^2}{s} \left(\frac{S_l^2}{\omega^2} - \Gamma_1 + \frac{c^2}{g} \frac{\Gamma_1'}{\Gamma_1} + \frac{c^2}{g} \frac{d}{dr} \right) U, \quad (21)$$

$$\begin{aligned} \frac{d\xi_r}{dr} &= \frac{1}{g} (\omega^2 - g') \xi_r + \left(1 - \Gamma_1 + \frac{c^2}{g} \frac{\Gamma_1'}{\Gamma_1} + \frac{c^2}{g} \frac{d}{dr} \right) U, \\ s &= 4\omega^2 r g - l(l+1)g^2 + \omega^2 r^2 (\omega^2 - 4\pi G \rho). \end{aligned}$$

$S_l^2 = \frac{l(l+1)}{r^2} c^2$ is the squared Lamb frequency and $N^2 = g \left(\frac{1}{H} - \frac{g}{c^2} \right)$ is the squared Brunt-Vaisala frequency. Inserting the first of Eqs. (21) into the second one, we eliminate ξ_r and obtain an ordinary differential equation of second order in $U(r)$:

$$U''(r) + f_1 U'(r) + f_2 U = 0, \quad (22)$$

$$f_1(r) = \frac{4}{r} + \frac{(\rho c^4)'}{\rho c^4} - \frac{s'}{s} = \frac{1}{H} + \varepsilon_1,$$

$$f_2(r) = \frac{\omega^2}{c^2} \left[1 - \frac{S_l^2}{\omega^2} \left(1 - \frac{N^2}{\omega^2} \right) \right] + \varepsilon_2,$$

$$\begin{aligned} \varepsilon_2 &= \frac{1}{c^2} \frac{S_l^2}{\omega^2} \left(8\pi G \rho - 4 \frac{g}{r} - g \frac{s'}{s} \right) \\ &+ \frac{1}{H_p} \left[\left(1 - H_p \frac{\Gamma_1'}{\Gamma_1} \right) \frac{s'}{s} \right. \\ &+ \frac{2}{r} \left(\frac{2}{\Gamma_1} - 1 + 2H_p \frac{\Gamma_1'}{\Gamma_1} \right) - \frac{4\pi G \rho}{g \Gamma_1} (1 + \Gamma_1) \\ &\left. + H_p \frac{\Gamma_1'}{\Gamma_1} \left(\frac{1}{H} - \frac{2}{H_p} + \frac{\Gamma_1''}{\Gamma_1} \right) \right], \end{aligned}$$

$$\frac{1}{H_p} = -\frac{1}{p} \frac{dp}{dr} = \Gamma_1 \frac{g}{c^2}.$$

Unless stated otherwise the prime will denote a derivative: $U'(r) = \frac{dU}{dr}$. The second order differential equation for the variable $U(r)$ has already been derived by Lamb (1932) for the propagation of small-amplitude spherical waves in an atmosphere with $g = \text{const}$, $\Gamma_1 = \text{const}$, and without curvature effects. Our Eq. (22) is a generalized Lamb equation, including curvature effects, especially close to the core of the Sun. Our purpose is to consider the eigenvalue problem for Eq. (22).

The theory of eigenvalues is usually based on a consideration of a homogeneous equation of the form

$$\check{L}U(r) = \omega^2 B(r)U(r), \quad (23)$$

where for an equation of second order the operator is

$$\check{L}U = a_2(r)U''(r) + a_1(r)U'(r) + a_0(r)U(r),$$

where $a_j(r)$ are smooth functions. A solution of the eigenvalue problem provides the eigenfunctions $U(r) \neq 0$ and eigenvalues ω^2 satisfying the linear differential Eq. (23) and the given

boundary conditions. With real coefficients $a_j(r)$, and under the conditions $a_2(r) \neq 0$ and $a_1(r) = a_2'(r)$ the eigenvalue problem with linear boundary conditions of the type:

$$\begin{aligned}\alpha_1 U(r_1) + \beta_1 U'(r_1) &= 0, \\ \alpha_2 U(r_2) + \beta_2 U'(r_2) &= 0,\end{aligned}\quad (24)$$

$|\alpha_1| + |\beta_1| > 0$, $|\alpha_2| + |\beta_2| > 0$, $\alpha_{1,2} = \text{const}$, $\beta_{1,2} = \text{const}$, is turned into a self-adjoint (Hermitian) problem of the Sturm-Liouville type, where $[r_1, r_2]$ is the integration interval. For the Sturm-Liouville problem the eigenvalues ω^2 are always real. Our boundary value problem on the base of Eq. (22) cannot to be turned into a Sturm-Liouville problem due to a singularity at the center $r = 0$ and at $r = r_s$, where $s(r_s) = 0$. This means that, as we will show below, near the central singularity ($r \rightarrow 0$) the solutions exhibit a power-law behavior ($\sim r^l$) but not an exponential one which is required for boundary conditions (24). Besides, for this problem the coefficients of the operator \tilde{L} are functions of the spectral parameter ω^2 . When the operator \tilde{L} depends on the spectral parameter ω^2 , the problem is hard to solve. For some special cases, this problem has been considered by e.g. Tamarkin (1928), Langer (1930), and Keldish (1951). As a consequence of that our linear eigenvalue problem formulated by Eq. (22) and by appropriate physical boundary conditions should generally have a spectrum with a set of complex values ω^2 .

It is convenient to define:

$$Y(r) = \frac{\sqrt{\rho c^2 r^2}}{\sqrt{s}} U(r).\quad (25)$$

Then, from Eq. (22) we get our basic equation:

$$Y''(r) + (K^2 + \varepsilon) Y(r) = 0,\quad (26)$$

where:

$$\begin{aligned}K^2 &= \frac{\omega^2}{c^2} \left[1 - \frac{\omega_c^2}{\omega^2} - \frac{S_l^2}{\omega^2} \left(1 - \frac{N^2}{\omega^2} \right) \right], \\ \omega_c^2 &= \frac{c^2}{4H^2} \left(1 - 2 \frac{dH}{dr} \right), \\ \varepsilon &= \varepsilon_2 - \frac{\varepsilon_1}{4} \left(\frac{2}{H} + \varepsilon_1 \right) - \frac{1}{2} \varepsilon_1'(r).\end{aligned}\quad (27)$$

For the integration of this equation we need $K^2(r)$ and $\varepsilon(r)$ profiles. We have used a standard model of the internal structure of the Sun (Stix, private communication; Stix & Skaley 1990) and the semi-empirical atmosphere model VAL3C of Vernazza et al. (1981). A combined model for the Sun, valid from the center up to the corona, was constructed by a smooth fitting of both models at the depth $r/R_\odot \approx 0.9971$. In this procedure we fitted the thermodynamic variables and their first and second derivatives which are required in Eq. (26). The extrapolation of the atmospheric model to the upper CCTR and the lower corona regions has been done using the method developed by Staude (Staude 1985; Obridko & Staude 1988). The solar 'surface' $r = R_\odot$ is defined at the photospheric depth where $T = T_{\text{eff}} = 5770$ K, that is at an optical depth of $\tau_0 \approx 0.3$.

To describe the dependence of the variables on height, we use another local atmospheric coordinate system with the axis \vec{z} directed upwards from the surface of the Sun. Thus we have $r = R_\odot + z$. The normalized independent variables are $r_* = 1 + \frac{h}{R_\odot} z_*$, where $r_* = \frac{r}{R_\odot}$ and $z_* = z/h$. Here $h = 2176$ km is the geometrical extent of the VAL3C model from the surface of the Sun.

In the asymptotic theory of solar p -modes Eq. (26) is usually applied without ε , i.e. it is assumed that $|K^2| \gg |\varepsilon|$ (Gough 1986; Christensen-Dalsgaard 1994). The solution is derived for the equation $Y'' + K^2(r)Y = 0$, where the condition $K^2(r_t) = 0$ defines the turning points, that means the boundaries of the p -mode cavity. Let us estimate the accuracy of such an assumption. Near the solar center ($r \rightarrow 0$), where $\rho \approx \rho_\odot = 150$ g/cm³, $4\pi G\rho_\odot \approx 2 \times 10^{-4}$ s⁻², $g \approx 4\pi\rho_\odot Gr/3$, we obtain $4\pi G\rho_\odot/\omega^2 \sim 1$ for the 5-min oscillations. So, $s \approx \omega^4 r^2$ for $l = 0$ and $s \approx -\omega^4 r^2 l^2$ for $l \neq 0$.

Near the solar surface ($r \rightarrow R_\odot \simeq 7 \times 10^5$ km), where $g \approx \text{const}$, $\rho \lesssim 10^{-8}$ g/cm³, and $4\pi G\rho/\omega^2 \lesssim 10^{-11}$, we have $s \approx \omega^4 R_\odot^2$ for $l \lesssim 10^3$. Hence it follows, that for small l the function $s(r)$ cannot be null, but for large l the function $s(r)$ changes its sign and has a zero at $r = r_s$. In Fig. 1a the function $s(r, l)$ is shown for $\omega = 2 \times 10^{-2}$ s⁻¹. It is clear, that inside the Sun $s \neq 0$ for $l < 20$, but there exists a zero of the function $s(r)$ near the center of the Sun for large $l \geq 20$. With increasing l this zero is shifted towards the solar surface. For instance, for $l = 20$ we have $r_s \sim 0.15R_\odot$, but $r_s \sim 0.75R_\odot$ for $l = 500$. We have a zero of the function $s(r)$ in the atmosphere for $l > 1000$.

The condition $s(r_s) = 0$ defines an internal singularity of Eq. (26). Thus, the assumption that Eq. (26) for $Y(r)$ has no singularity (Gough 1986; Christensen-Dalsgaard 1994), is correct for $l \lesssim 20$ only.

In Fig. 1b the relation $|\varepsilon/K^2|$ for the 5-min oscillations is shown. We can see that the contribution of $\varepsilon(r)$ in Eq. (26) becomes significant close to the zeros of the functions $K^2(r)$ and $s(r)$. In the outer part of the Sun this ratio is small ($\sim 3 \cdot 10^{-2}$) for all $l < 10^3$. Hence only in a qualitative analysis the function $\varepsilon(r)$ can be omitted in Eq. (26) in comparison with $K^2(r)$.

In the outer part of the Sun ($r \geq R_\odot$) we have $K^2 \approx (\omega^2 - \omega_c^2)/c^2$ for low l . So the solution is defined by the cut-off frequency and the behavior of the solution depends on the sign of the difference $\omega^2 - \omega_c^2$. For $\omega^2 > \omega_c^2$ the solution will oscillate. But for $\omega^2 \leq \omega_c^2$ we get an evanescent behavior. If the radial widths of the oscillatory and the evanescent zones are finite we will call them cavity (transparent) and tunnel (opaque), respectively. For a fixed frequency and wave number a tunnel is located between two cavities.

In Fig. 2 the height dependence of $\omega_c^2(z)$ is illustrated, showing clearly the influence of the chromosphere on the formation of the wave structure. In dependence on the gradient of the temperature some extrema arise in the function $\omega_c^2(z)$ and ω_c^2 becomes negative in the upper chromosphere where $T \approx 7000$ K as well as at the temperature plateau in the transition zone at $T \approx 23500$ K.

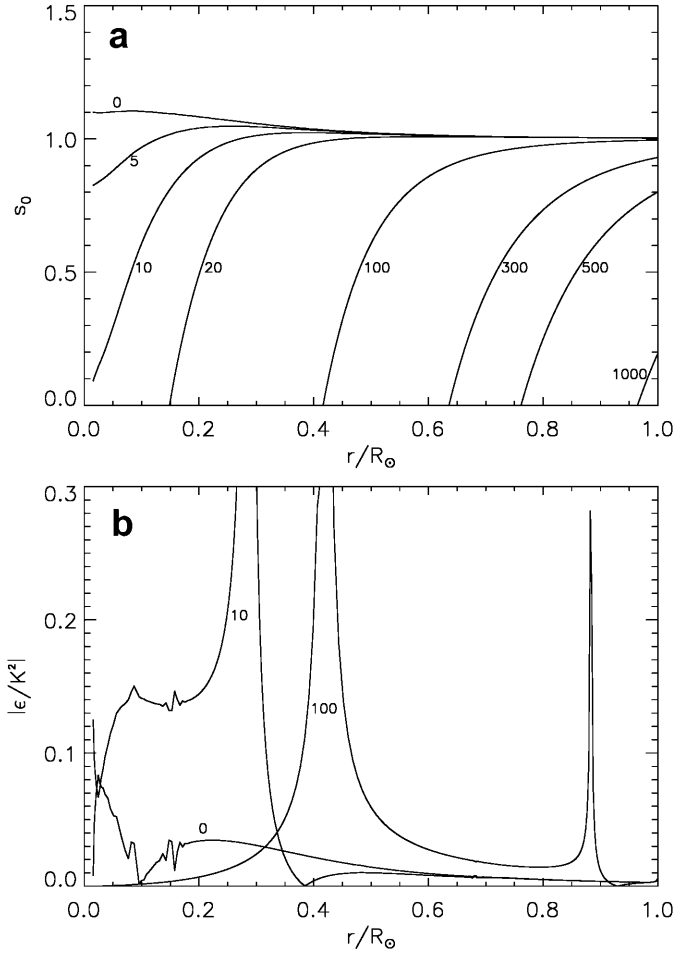


Fig. 1. **a** The function s_0 , where $s(r, l) = \omega^4 r^2 s_0(r, l)$, for $l = 0$ –1000 and $\omega = 2 \times 10^{-2} \text{ s}^{-1}$, plotted against the fractional radius r/R_\odot in the solar interior. **b** The function $\epsilon(r, l)$ (traditionally omitted in the governing equation) in comparison with $K^2(r, l)$ plotted against r/R_\odot for the cases $l = 0, 10, 100$ and $\omega = 2 \times 10^{-2} \text{ s}^{-1}$.

For all frequencies below 6 mHz an additional cavity exists at the base of CCTR. The width of this chromospheric cavity grows with frequency. Between the chromospheric cavity and the inner cavity the tunnel with a complex structure is located at the photosphere. For some frequencies (e.g., $\nu \sim 5.5$ mHz) an additional cavity with narrow width is possible in the region $0 \lesssim z/h \lesssim 0.15$. For higher frequencies ($\nu \geq 6.5$ mHz) the atmospheric tunnel disappears at all and the waves can propagate through the atmosphere up to CCTR.

To account for the damping we admit complex frequencies $\omega = \omega_1 - i\omega_2 = \omega_1(1 - i\eta)$, $\eta > 0$,

$$(28)$$

where the imaginary part of the frequency $\omega_2 > 0$ causes a decay of the oscillations with the damping rate $\eta = \omega_2/\omega_1 \neq 0$. Now for $\eta \neq 0$ the problem of the singularity of Eq. (26), where $s(r_s) = 0$ at real ω , is not important for large l . As $\omega^2 = \omega_1^2(1 - \eta^2 - 2i\eta) \approx \omega_1^2(1 - 2i\eta)$, where the condition of small $\eta^2 \ll 1$ due to the tunnel effect is assumed (this assumption will be applied in all qualitative analyses), we get for the imaginary part of the function $s(r, \omega)$

$$\text{Im}\{s(r, \omega_1, \eta)\} = -r^2 \omega_1^2 4\eta \left(\omega_1^2 + \frac{g}{r} 2 - 2\pi G\rho \right). \quad (29)$$

It is clear that at $r \neq 0, \eta \neq 0$ we have $\text{Im}\{s(r)\} \neq 0$. That means, for complex frequencies ($\eta \neq 0$) the condition for the singularity $|s(r_s)| = 0$ is not satisfied for any ω or l .

4. Where are the turning points?

This problem was already considered in our earlier paper (Dzhililov & Staude 1995), where the tunneling of waves through the acoustic barrier into the atmosphere for non-trapped oscillations was investigated. It was shown that the waves penetrate into the barrier upwards to some height and remain progressive, which should extend the size of the inner acoustic cavity. Here, we shall consider a similar task, taking into account the existence of the turning points for the p -modes in the real solar model. The question arises, how do the turning points change by $\eta \neq 0$? Without the tunneling effect ($\eta = 0$) the turning points of Eq. (26) are defined by the roots of equation $K^2(r; l, \omega) = 0$ (Stix 1989). For high ω the condition $\omega^2 \approx S_l^2$ defines the level of the inner reflection:

$$r_t = \sqrt{l(l+1)}c(r_t)/\omega, \quad (30)$$

and $\omega^2 \approx \omega_c^2$ corresponds to the surface turning point for low l .

Here, our qualitative analysis will be done without the corrections connected with the term $\epsilon(r)$ in Eq. (26). For $\eta \neq 0$ two types of turning points exist:

1. $\text{Re}\{K^2(r)\} = \text{Im}\{K^2(r)\} \equiv 0$ — a ‘total’ turning point;
2. $\text{Re}\{K^2(r)\} \neq 0, \text{Im}\{K^2(r)\} = 0$ — a ‘transition’-type turning point.

While constructing the solutions of Eq. (26) we shall see, why these equations define the turning points. Now we consider, at which circumstances these conditions are met. Instead of the conditions $\text{Re}\{K^2\} = 0$ and $\text{Im}\{K^2\} = 0$ we can write the equations:

$$\omega_1^2 - \omega_2^2 - \omega_c^2 - S_l^2 + S_l^2 N^2 \frac{\omega_1^2 - \omega_2^2}{(\omega_1^2 + \omega_2^2)^2} = 0, \quad (31)$$

$$\frac{S_l^2 N^2}{(\omega_1^2 + \omega_2^2)^2} = 1. \quad (32)$$

Eq. (32) is a necessary condition for the existence of both types of turning points. From this condition it follows immediately that a turning point cannot be located in the convective zone as $N^2 > 0$ must be fulfilled. The solutions of Eqs. (31, 32) for ω_1^2 and ω_2^2 yield

$$\begin{aligned} 4\omega_1^2 &= 2S_l N + S_l^2 + \omega_c^2 > 0, \\ 4\omega_2^2 &= 2S_l N - S_l^2 - \omega_c^2 \geq 0. \end{aligned} \quad (33)$$

For the radial modes ($S_l = 0$) these equations change into $4\omega_1^2 = \omega_c^2$ and $4\omega_2^2 = -\omega_c^2$. This means, that for radial modes the necessary condition for the turning points is not obeyed. For nonradial modes $l \neq 0$ the conditions Eq. (33) might be fulfilled if

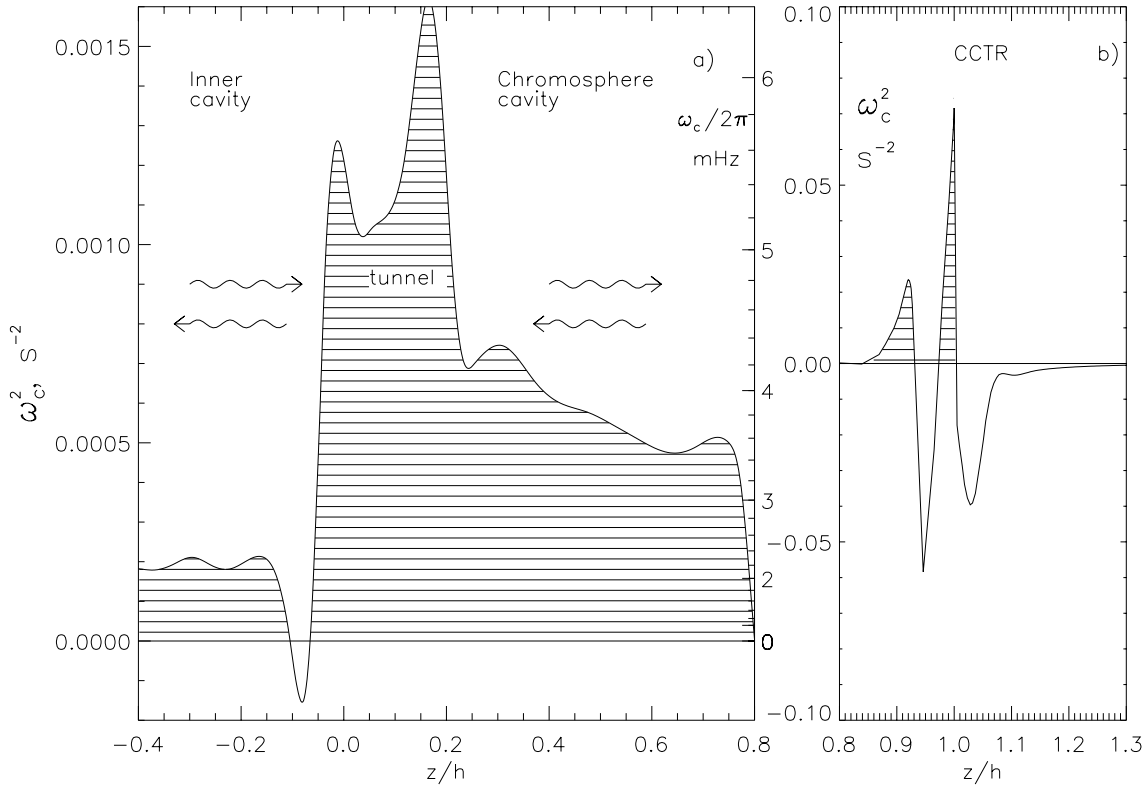


Fig. 2. Dependence of the squared cut-off frequency on the height (normalized to $h = 2176$ km) of the atmospheric model VAL3C. The hatched domains are evanescent zones through which a tunneling of waves occurs. The wide chromospheric cavity a) and the narrow CCTR cavity b) arise due to the sharp temperature gradients in the atmosphere. The right-hand ordinate gives $\omega_c/2\pi$ in mHz to identify the boundary of the opaque zone for a given frequency of the p -modes. The surface of the Sun ($r = R_\odot$) corresponds to $z = 0$.

$$0 < A \leq 1, \text{ where } A \equiv \frac{S_l^2 + \omega_c^2}{2S_l N}. \quad (34)$$

Fig. 3a shows regions where this condition is satisfied. For $l \leq 10$ the curves cross the dashed $0 < A \leq 1$ area always at the base of the convection zone, $r_* \sim 0.68$. However, determining $\omega_1 = 2\pi\nu$ for $l \leq 10$ at $r_* \sim 0.68$ from Eq. (33), we get $\nu < 0.6$ mHz. This means, that a ‘total’ turning point for the p -modes cannot exist in the solar interior. Only for g -modes this condition can be met at the lower boundary of the convective zone.

Fig. 3b illustrates a dependence of A on the height z in the solar atmosphere. For all l the curves cross the line $A = 1$ four times in the region extending from the upper chromosphere to CCTR. The estimate of ω_1 from Eqs. (33) shows that for the whole frequency range of p -modes (2–10 mHz) the ‘total’ turning points can be located in CCTR.

4.1. Upper turning point

So far we proved that condition (34) for the existence of ‘total’ turning points is satisfied in the upper solar atmosphere only. Where are these points located?

In Fig. 4 the curves for the quantities $A_1 = 4\omega_1^2 - (2S_l N + S_l^2 + \omega_c^2)$ and $A_2 = 4\omega_2^2 - (2S_l N - S_l^2 - \omega_c^2)$ which follow from Eq. (33) are shown. The crossings of these

curves at their zeros ($A_1 = A_2 = 0$) correspond to three ‘total’ turning points which occur at the boundaries between CCTR barriers and the cavities (see Fig. 2b). Sharp changes of the functions $A_{1,2}(z)$ near their zeros are responsible for the existence of turning points for all frequencies $\nu \leq 10$ mHz, while $\eta^2 < 1$ there. For frequencies $\nu < 10$ mHz the positions of the turning points are practically independent of ν and l . They are defined by the positions of the strong temperature gradients and the plateau of T in the upper chromosphere and CCTR. Approximately, these points are settled at the levels where $\frac{d}{dz} \frac{1}{H} \approx 0$. These levels are very close to those where $T'''(z) \simeq 0$.

We must emphasize that we defined the places of three ‘mathematical’ turning points which obey Eq. (33). We will see further that as a consequence of tunneling the only physically justifiable point is the last one, $r = r_a$, that is close to the corona and not connected with the existence of a temperature plateau. Nevertheless, the cascading character of the upper turning points in the CCTR creates favorable conditions for the accumulation of wave energy in a very narrow layer. This accumulation can be of great interest for heating the upper atmosphere.

4.2. Lower turning point

Let us now consider a formation of ‘transition’-type turning points which are defined by the equation $\text{Im}(K^2 + \varepsilon) = 0$. For

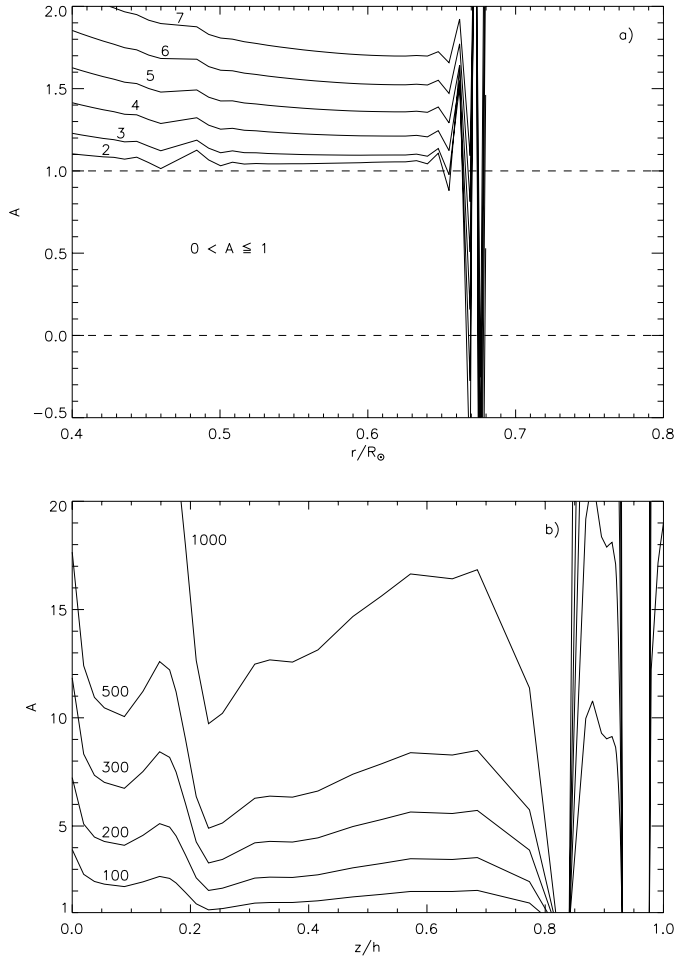


Fig. 3a and b. Check of the necessary condition $0 < A \leq 1$, Eq. (34), for the existence of ‘total’ turning points: **a** inside the Sun, **b** in the atmosphere. For the p -modes this condition is satisfied in the upper atmosphere, at the region $0.8 \leq z/h \leq 0.95$ only.

this purpose we have to investigate the behavior of the function $(K^2 + \varepsilon)$ near the solar center. We write the density at $r \rightarrow 0$ in the following way:

$$\rho \approx \rho_{\odot} \left[1 - b \left(\frac{r}{R_{\odot}} \right)^d \right], \quad (35)$$

where $\rho_{\odot} \approx 150 \text{ g/cm}^3$ is the density in the solar center and d and b are constants. From the solar model it follows that for $r \rightarrow 0$ we have $\rho'(r) \rightarrow -0$ and $-\rho''(r) \neq 0$. Hence, d has to satisfy the condition $1 < d \leq 2$. Comparing Eq. (35) with the real model near the center, we get $d = 1.938$ and $b = 59.448$. The remaining quantities can be found as follows:

$$\frac{1}{H} \approx \frac{db}{R_{\odot}} \left(\frac{r}{R_{\odot}} \right)^{d-1}, \quad g \approx g'r,$$

$$g'(r) = \frac{4\pi}{3} G \rho_{\odot} = 4.192 \times 10^{-5} \text{ s}^{-2}, \quad \frac{N^2}{g} \rightarrow +0.$$

Using these approximations we get

$$\varepsilon \approx -\frac{1}{rH} \left(1 + \frac{3}{2} \frac{\beta}{1 - \beta^2 L + O(\eta^2)} \right), \quad (36)$$

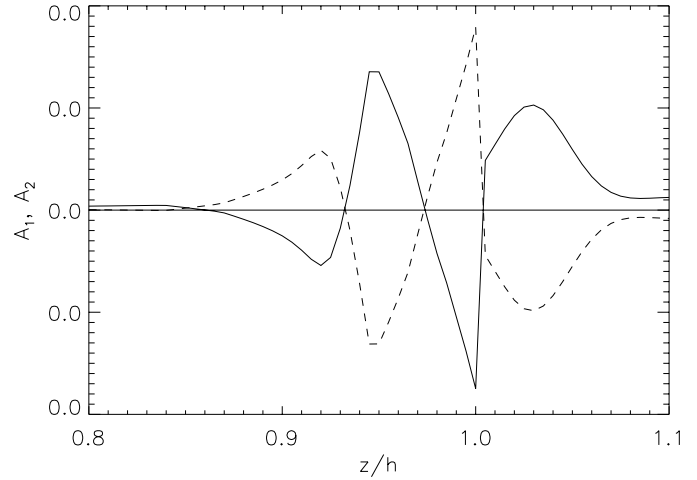


Fig. 4. The locations of the upper turning points in CCTR, determined by the conditions $A_1 = 0$ (solid curve) and $A_2 = 0$ (dashed curve). The crossings of these curves display the places of the turning points which are valid for the whole range of frequencies of the p -modes.

where $\beta = \frac{g'}{\omega^2} \approx \beta_0 (1 + 2i\eta)$, $\beta_0 = \frac{4\pi G \rho_{\odot}}{3\omega_1^2} \leq 10^{-1}$, and $L = l(l+1)$. Then, we get

$$\lim_{r \rightarrow 0} (K^2 + \varepsilon) \approx -\frac{L}{r^2} - \frac{3}{2} \frac{1}{rH} - 2i\eta \frac{\omega_1^2}{c^2} \left(1 - \frac{S_l^2 N^2}{\omega_1^4} \mu_* \right), \quad (37)$$

where $\mu_* \approx 1 - \frac{3}{2L} \frac{1 + L\beta_0^2}{(1 - L\beta_0^2)^2 + O(\eta^2)}$, if $|1 - L\beta_0^2| \geq 1$.

Near the points, where $\text{Re}\{s\} \approx 0$, i.e. $|1 - L\beta_0^2| < 1$, we have $\mu_* \approx 1$. It is clear that for all $l \neq 0$, μ_* is positive and $\mu_* \approx 1$. By this way the lower turning point is practically defined by the condition

$$\omega_1^4 \approx S_l^2 N^2. \quad (38)$$

Thus the condition $\text{Im}\{K^2\} = 0$ is defined practically by the real part of the frequency ω_1 . For the 5-min oscillations ($\nu = 3.33 \text{ mHz}$) the position of the inner turning point is shown in Fig. 5a. Here, the dotted curve corresponds to Eq. (30) (the case of $\eta = 0$), but the lower curve corresponds to Eq. (38) (the case of $\eta \neq 0$). It is clear that due to the tunneling effect the turning point lies closer to the solar center for lower l . For instance, for modes with $l = 100$ the position of the turning point changes from $0.9R_{\odot}$ to $0.3R_{\odot}$. Such a huge extension of the main cavity must strongly influence the eigenfrequencies. In Fig. 5b the positions of the turning points for different frequencies are shown as a dependence on l , corresponding to Eq. (38).

Thus, the p -modes are trapped in the region in which the lower reflection point is located below the convection zone for all l and ν . For low $l \leq 10$ this level is close to the solar center. For all l and ν the upper turning point is at CCTR.

It is noteworthy that the locations of the turning points can be changed only slightly, depending on the choice of the dependent variable for which the second-order differential equation is obtained from the initial set of wave equations. However, the turning points are determined in order to solve the eigenvalue

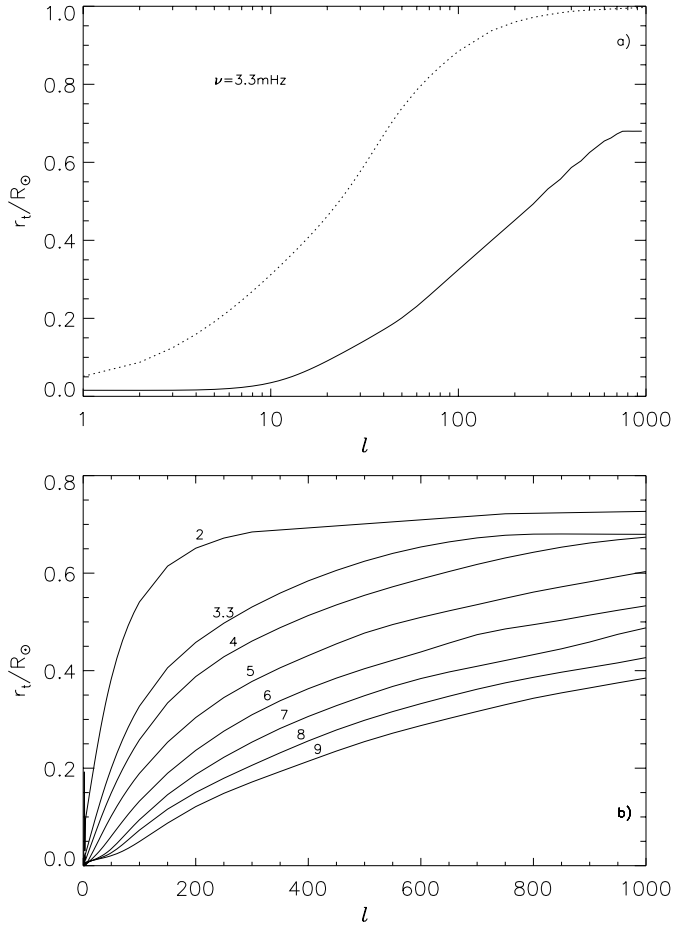


Fig. 5a and b. The location r_t/R_\odot of the inner turning point. The results are shown as functions of the degree l for different frequencies (in mHz) which are denoted by numbers at the curves. **a** the case of $\nu = 3.3$ mHz with $\eta = 0$ (without tunneling – dotted line) and $\eta \neq 0$ (with tunneling – solid line). **b** $r_t(l, \nu)$ for the case of $\eta \neq 0$.

problem and the eigenvalues (frequencies) of the initial system are invariant (Federuk 1983).

5. Asymptotic solution

In order to construct the asymptotic solution of Eq. (26) let us rewrite it in the standard form. Having in mind high frequencies of the p -modes we introduce the formal large spectral parameter λ and the radial distance r_* normalized to R_\odot :

$$\begin{aligned} \lambda^2 &= \frac{R_\odot^2 \omega_1^2}{c_\odot^2}, \quad r_* = \frac{r}{R_\odot}, \\ R_\odot^2 K^2 &= \lambda^2 Q = \lambda^2 (Q_r - iQ_i), \\ R_\odot^2 \varepsilon &= \lambda^2 (\varepsilon_r - i\varepsilon_i), \\ Q_r &= \frac{c_\odot^2}{c^2} \left[1 - \eta^2 - \frac{\omega_c^2}{\omega_1^2} - \frac{S_l^2}{\omega_1^2} + \frac{S_l^2 N^2}{\omega_1^4} \frac{1 - \eta^2}{(1 + \eta^2)^2} \right], \\ Q_i &= 2\eta \left[1 - \frac{S_l^2 N^2}{\omega_1^4 (1 + \eta^2)^2} \right] \frac{c_\odot^2}{c^2}, \end{aligned} \quad (39)$$

$$\varepsilon_r = \frac{c_\odot^2}{\omega_1^2} \operatorname{Re}\{\varepsilon\}, \quad \varepsilon_i = -\frac{c_\odot^2}{\omega_1^2} \operatorname{Im}\{\varepsilon\}.$$

In particular for $\eta^2 \ll 1$ we have

$$Q_r \approx \frac{c_\odot^2}{c^2} \left(1 - \frac{\omega_c^2}{\omega_1^2} - \frac{S_l^2}{\omega_1^2} + \frac{S_l^2 N^2}{\omega_1^4} \right), \quad (40)$$

$$Q_i \approx 2\eta \frac{c_\odot^2}{c^2} \left(1 - \frac{S_l^2 N^2}{\omega_1^4} \right). \quad (41)$$

Here, $c_\odot = \text{const}$ is the sound speed defined at the solar surface. Henceforth, for convenience purposes the subscript $*$ at r_* will be omitted. Instead of Eq. (26) we have now the main equation

$$Y''(r) + \lambda^2 q(r; \lambda^{-2}, \eta) Y(r) = 0 \quad (42)$$

with $q = Q_r + \varepsilon_r - i(Q_i + \varepsilon_i) = q_r - iq_i$. For the range of p -mode frequencies $\lambda \simeq 10^3$. As a consequence of that Eq. (42) contains a large parameter $\lambda \gg 1$. A study of this equation is cumbersome because $q(r, \omega)$ is a complex-valued function. In the case of $\eta = 0$ the turning points of Eq. (42) are determined by the zeros of $Q_r(r)$ (if some corrections due to the function $\varepsilon(r)$ are excluded). In our case when $\eta \neq 0$ the turning points are defined by both functions Q_r and Q_i . Setting $q \simeq \text{const}$ the linear independent solutions of Eq. (42) are expressed by $Y_{1,2} = \exp(\pm i\lambda\sqrt{q}r)$. For the more realistic case of $q \neq \text{const}$ the formal asymptotic solutions should be looked for (Federuk 1983)

$$Y = \exp\left(\int^r \sum_{k=-1}^{\infty} \lambda^{-k} \alpha_k(r) dr\right). \quad (43)$$

The substitution $W = \frac{Y'}{Y}$ transforms Eq. (42) to the Riccati equation

$$W' + W^2 + \lambda^2 q(r) = 0. \quad (44)$$

Putting Eq. (43) into Eq. (44) yields

$$\sum_{k=-1}^{\infty} \lambda^{-k} \alpha_k'(r) + \left(\sum_{k=-1}^{\infty} \lambda^{-k} \alpha_k(r) \right)^2 + \lambda^2 q(r) = 0. \quad (45)$$

Setting the coefficients of degree λ^{-k} to zero, we get a set of recurrent equations for the functions $\alpha_{-1}(r), \alpha_0(r), \alpha_1(r), \dots$. The first equation from this set is $\alpha_{-1}^2 = -q$. Hence $\alpha_{-1} = \pm i\sqrt{q}$. With $\alpha_{-1} = +i\sqrt{q}$ we get

$$\alpha_{-1}(r) = i\sqrt{q}, \quad \alpha_0(r) = -\frac{q'}{4q}, \quad i\alpha_1(r) = \frac{1}{8} \frac{q''}{q^{3/2}} - \frac{5}{32} \frac{q'^2}{q^{5/2}}. \quad (46)$$

For all functions $\alpha_k(r)$ the recurrent relation may be written as

$$\alpha_{k+1}(r) = \frac{i}{2\sqrt{q}} \left[\alpha_k'(r) + \sum_{j=0}^k \alpha_j(r) \alpha_{k-j}(r) \right]. \quad (47)$$

In the case of $\alpha_{-1} = -i\sqrt{q}$ in the last two formulae \sqrt{q} must be replaced by $-\sqrt{q}$. So, Eq. (42) has two asymptotic solutions

$$Y_{1,2} = \frac{1}{4\sqrt{q}} \exp\left[\pm i\lambda \int^r \sqrt{q} dr\right]$$

$$+ \sum_{k=1}^{\infty} (\pm\lambda)^{-k} \int^r \alpha_k(r) dr]. \quad (48)$$

These solutions are not valid at the turning point $r = r_a$, where $q_r = q_i = 0$. At this point the roots of the characteristic equation $p^2 - q(r) = 0$ coincide. The existence of the branch $\text{Re}\left\{\sqrt{q(r)}\right\} \geq 0$ in the complex domain is supposed. To solve the boundary value problem we must determine a small spectral parameter η . As a consequence of that the second terms of degree λ^{-1} in the asymptotic solutions should be retained. Let

$$P(r) = 1 - \frac{1}{8\lambda^2 q} \left(\frac{q''}{q} - \frac{5}{4} \frac{q'^2}{q^2} \right) + O(\lambda^{-3}). \quad (49)$$

Then, the solutions may be written as

$$Y_{1,2} \simeq q^{-1/4} \exp\left(\pm i\lambda \int^r \sqrt{q} P(r) dr\right). \quad (50)$$

$P = 1$ corresponds to the main branch of the asymptotic solutions.

The asymptotic solutions of Eq. (42) which are valid at the turning point $r = r_a$ are derived in the Appendix.

6. Boundary value problem

On the basis of the derived asymptotic solutions a global solution of Eq. (42) can be constructed. This solution must be regular over the whole range of integration region, $0 \leq r \leq \infty$.

6.1. Solar center

Near the solar center, where $r \rightarrow 0$, Eq. (37) can be used and Eq. (26) is simplified. For radial waves both solutions of this equation are regular at the center of Sun. Hence, the radial waves are reflected from the center of the Sun. In the case of nonradial waves $l \neq 0$ the solutions are

$$Y \approx \tilde{C}_1 r^{1+l} + \tilde{C}_2 r^{-l}. \quad (51)$$

The requirement of regularity of the solutions at the center ($r \rightarrow 0$) results in $\tilde{C}_2 = 0$. This means that there is a turning point at $r = r_t$ for the nonradial waves. This point is connected with the appearance of the singularity at the Sun's center. The location of this point is defined by Eq. (38). In the global solution, in the region $r \leq r_t$, one solution must be retained only. This solution describes the waves decreasing in amplitude and running toward to center of the Sun. At $r \geq r_t$ the common solution must include both solutions: downgoing waves and outwardly propagating waves which are reflected from $r = r_t$.

Now we write the common solution of Eq. (42) for both cases $l = 0$ and $l \neq 0$ in the form

$$Y \approx q^{-1/4} \left[C_1 e^{i\lambda \int_{r_t}^r \sqrt{q} P(r) dr} + C_2 e^{-i\lambda \int_{r_t}^r \sqrt{q} P(r) dr} \right]. \quad (52)$$

For the *radial* waves we have $r_t \approx 0$, $C_{1,2} \neq 0$ in the solution and it is valid for the whole range of r including $r = r_a$. As the radial waves are reflected totally from the center we

can apply a rigid boundary condition at the center ($r \rightarrow 0$): $\xi_r(0) = 0$. It follows from the first of Eq. (21) that at $r \approx 0$ we have $U'(r) \approx -\omega^2 \xi_r / c^2$. So, for radial waves the boundary condition at the center is

$$\left[\frac{dU}{dr} \right]_{r \rightarrow 0} = 0. \quad (53)$$

As for $r \rightarrow 0$ we have $\rho \approx \text{const}$, $c^2 \approx \text{const}$, $\sqrt{s} \sim r$ it follows from Eq. (25) that $Y(r) \approx \text{const} \cdot rU$. Then, from Eq. (53) we have $rY'(r) - Y(r) = 0$. Since $Y'(r)$ is finite at $r = 0$ we have

$$Y(0) = 0. \quad (54)$$

Fitting Eq. (52) to this boundary condition, we have finally for radial waves

$$Y = \frac{C}{4\sqrt{q}} \sin\left(\lambda \int_0^r \sqrt{q} P(r) dr\right), \quad (55)$$

with only one integration constant $C = 2iC_1 = -2iC_2$.

For the *nonradial* waves $l \neq 0$ the second term of (52) is irregular at $r \rightarrow 0$ and hence $C_2 = 0$. Then, we have

$$Y \simeq \frac{C}{4\sqrt{q}} e^{i\lambda \int_{r_t}^r \sqrt{q} P(r) dr}. \quad (56)$$

Let us consider the behavior of this solution around the turning point $r = r_t$. In the case of $r \rightarrow r_t$ we have $q_i \approx q'_i(r_t)(r - r_t)$, $q_r(r_t) \approx \text{const}$, and $q'_i(r_t) > 0$. Hence, the main value of the solution ($P = 1$) of Eq. (56) becomes

$$Y \sim e^{i[\lambda_0(r-r_t)^2 - \omega_1 t] - \omega_2 t}, \quad (57)$$

where $\lambda_0 = \frac{\lambda q'_i(r_t)}{4|q_r(r_t)|^{1/2}} > 0$. It follows that a wave front is directed toward the center of the Sun for $r < r_t$. For $r > r_t$, the wave front is directed toward the surface of the Sun. Here, $r = r_t$ is a transition point between the waves with different directions of propagation. Hence, the solution of Eq. (56) satisfies the central boundary condition for nonradial waves mentioned above, but it is not complete in the area $r \geq r_t$. For the last case the solutions are defined in the Appendix.

We constructed the solution for the radial waves. This solution is given by Eq. (55) which is valid for the whole interval of integration. Eq. (56) is appropriate for the nonradial waves. This solution is valid below the turning point $r \leq r_t$.

6.2. Upper atmosphere

To solve the boundary value problem a second boundary condition is required. At $r \rightarrow \infty$ the solution must be limited. In the case of $\eta = 0$ the surface of the Sun reflects the p -modes if the condition $\omega^2 \approx \omega_c^2$ is satisfied. In this case the exponential decrease of the wave amplitude in the atmosphere provides the second boundary condition. In the case of $\eta \neq 0$ the upper turning point does not exist for radial waves and a cascade of upper turning points located in CCTR arises for nonradial waves. In this case it is natural to suppose that the waves are reflected from the sharp gradient of CCTR when they partially pass to

the transparent corona as outwardly propagating waves. As the frequency and hence the radial wavenumber are complex let us consider in detail waves which propagate in the solar corona.

We consider an isothermal corona with the parameters $T \approx \text{const} \approx 2 \times 10^6$ K, $g = 0.274$ km/s², $\Gamma_1 \approx 5/3$; $c \approx 100$ km/s, $\rho = \rho_{00}e^{-r/H}$, $\frac{1}{H} = \frac{\Gamma_1 g}{c^2} \sim 5 \times 10^{-5}$ km⁻¹, $\omega_c^2 \approx 4 \times 10^{-6}$ s⁻², $N^2 \approx 6 \times 10^{-6}$ s⁻², $\frac{N^2}{\omega_1^2} \sim 10^{-2}$, $\frac{\omega_c^2}{\omega_1^2} \sim 10^{-2}$. Then, in the main equation $Y''(r) + \lambda^2 q Y(r) = 0$, $q = \text{const} = q_r - iq_i$, where for $r \rightarrow \infty$ we have

$$q_r \approx 1 - \frac{\omega_c^2}{\omega_1^2} \lesssim 1, \quad q_i \approx 2\eta > 0, \quad (58)$$

$$Y = \left(C_1 e^{i\lambda\sqrt{q}r} + C_2 e^{-i\lambda\sqrt{q}r} \right) e^{-i\omega_1 t} e^{-\omega_2 t}. \quad (59)$$

We remind that here the normalized $r \Rightarrow r_* = r/R_\odot$ is used. Taking into consideration that $\sqrt{q} \approx \sqrt{q_r} - \frac{i}{2} \frac{q_i}{\sqrt{q_r}}$ and requiring that in the corona only outgoing waves must be retained, i.e. $C_2 = 0$, we have

$$Y = C_1 \exp \left[i \frac{\omega_1}{c} (r - ct) + \frac{\omega_2}{c} \left(\frac{r}{q_r} - ct \right) \right]. \quad (60)$$

Hence, it follows that at $r \rightarrow \infty$ the wave amplitudes become infinite. Even for a coordinate system moving with the sound speed, $V_0 = c = r/t$, a scenario does not change for $q_r < 1$. As a consequence of that linear waves cannot penetrate into the isothermal corona. Similar conclusions can be drawn for a non-isothermal corona.

Gouttebroze et al. (1999) and Steffens & Deubner (1999) have analyzed the velocity and intensity of oscillations in more than 15 spectral lines. As they did not find any evidence of oscillations for lines formed at temperatures higher than 5×10^5 K they concluded that the waves in the range 2–7 mHz are entirely reflected (or dissipated) by CCTR.

As a consequence of that another boundary condition should be applied in CCTR. A total reflection of waves from CCTR will not be employed, because the corona is not an evanescent infinite waveguide. It will be shown later that a flux of energy of waves tunneling through the upper boundary is possible.

The transition from the chromosphere to the corona is accompanied by a sharp decrease of the density by a factor of 100. In such a case it is more natural to consider CCTR as a free surface, similar to the surface of the ocean. At a free surface the pressure will not be changed: $\frac{dp(r,t)}{dt} = 0$ which corresponds to $p' = \rho_0 g \xi_r$. Taking this condition at CCTR, from Eq. (20) we have $U = 0$. In a reality spherical surface gravity waves might be forced at the free surface. For the free surface gravity waves (f -modes) the condition $U = 0$ is satisfied and the dispersion relation is $\omega^2 = gk_\perp$. For forced f -modes the dispersion relation will be slightly changed and $U \neq 0$. In this part of the paper we will restrict ourself to the condition $U = 0$ at the surface. Hence, from Eq. (25) we have a second boundary condition

$$Y|_{r=r_a} = 0, \quad (61)$$

where the normalized $r_a \approx 1 + \frac{h}{R_\odot}$. Taking into account this condition in Eq. (55), we obtain a complex integral eigenvalue equation for the radial modes:

$$\lambda \int_0^{r_a} \sqrt{q} P(r) dr = n\pi. \quad (62)$$

Here, n is the radial order of the p -modes.

Now let us consider the nonradial modes. The solution of Eq. (42) which is valid at the upper total turning point is presented in the Appendix; it may be written as

$$Y = E_1 \frac{A_i(-x)}{\sqrt{x'(r)}} \left[1 - \Phi_0 \frac{A_i'(-x)}{A_i(-x)} \right] + E_2 \frac{B_i(-x)}{\sqrt{x'(r)}} \left[1 - \Phi_0 \frac{B_i'(-x)}{B_i(-x)} \right], \quad (63)$$

where $x = \left(\frac{3}{2}\zeta\right)^{2/3}$, $\zeta = \lambda \int_r^{r_a} \sqrt{q} dr$, the function $\Phi_0(x(r))$ is defined in the Appendix (Eq. (A29)) and $E_{1,2} = \text{const}$. Substituting Eq. (63) into Eq. (61) we define the relation between E_1 and E_2 :

$$\frac{E_1}{E_2} = -\sqrt{3} \frac{1 - \sigma\Phi_{00}}{1 + \sigma\Phi_{00}}. \quad (64)$$

To obtain this relation for $r \rightarrow r_a$, $x(r_a) \rightarrow 0$, $x'(r_a) \neq 0$, $\Phi_{00} = \Phi_0(r_a) \sim \lambda^{-4/3}$ and $\frac{B_i'(0)}{B_i(0)} = -\frac{A_i'(0)}{A_i(0)} = \sigma = \sqrt[3]{3} \frac{\Gamma(2/3)}{\Gamma(1/3)}$ are taken, where $\Gamma(a)$ is the Gamma function. Substituting the relation E_1/E_2 into Eq. (63) and taking into account the relation between Airy and Bessel functions (Abramowitz & Stegun 1984), we get

$$Y = E \sqrt{\frac{x}{x'(r)}} \left\{ J_{1/3}(\zeta) - \sigma\Phi_{00} J_{-1/3}(\zeta) + \Phi_0 \sqrt{x} [J_{-2/3}(\zeta) + \sigma\Phi_{00} J_{2/3}(\zeta)] \right\}, \quad (65)$$

where $E = \text{const}$. Eq. (65) defines the eigenfunctions of the non-radial waves if the eigenfrequencies are known. To derive the dispersion equation for frequencies we have to match Eq. (65) with Eq. (56) at the lower turning point $r = r_t$. Since we have $|\zeta| \gg 1$ for $r \rightarrow r_t$ the asymptotic presentation of the Bessel functions for large arguments may be used. At $|\arg(\zeta)| < \pi$

$$J_m(\zeta) \approx \sqrt{\frac{2}{\pi\zeta}} \left[\cos(\gamma_m) - \frac{4m^2 - 1}{8\zeta} \sin(\gamma_m) \right], \quad (66)$$

where $\gamma_m = \zeta - \frac{\pi}{4} - m\frac{\pi}{2}$.

Then for Eq. (65) and its first derivative we obtain

$$Y(r) \simeq E \sqrt{\frac{x}{x'(r)}} \sqrt{\frac{2}{\pi\zeta}} \left(\cos \gamma + \frac{a_1}{\zeta} \sin \gamma \right), \quad (67)$$

$$Y'(r) \simeq E \sqrt{\frac{x}{x'(r)}} \sqrt{\frac{2}{\pi\zeta}} \left(\sin \gamma + \frac{a_2}{\zeta} \cos \gamma \right) \cdot \lambda \sqrt{q},$$

$$\gamma(r) = \zeta(r) - \frac{5\pi}{12},$$

$$a_1 = \frac{5}{72} - \sqrt{x}\Phi_0\zeta, \quad a_2 = \frac{7}{72} + \sqrt{x}\Phi_0\zeta - \frac{\zeta}{\lambda\sqrt{q}} \frac{x''(r)}{2x'(r)}.$$

Here, we retained the first two terms in λ^{-1} . The parameters $a_{1,2} \sim \lambda^0$. From the continuity condition of the solutions and their derivatives at $r = r_t$ a set of algebraic equations is derived

$$E \sqrt{\frac{x}{x'(r)}} \sqrt{\frac{2}{\pi\zeta}} \left(\cos \gamma + \frac{a_1}{\zeta} \sin \gamma \right) = \frac{C}{\sqrt[4]{q}}, \quad (68)$$

$$E \sqrt{\frac{x}{x'(r)}} \sqrt{\frac{2}{\pi\zeta}} \left(\sin \gamma + \frac{a_2}{\zeta} \cos \gamma \right) = ib \frac{C}{\sqrt[4]{q}},$$

where $b = 1 + i \frac{q'(r_t)}{4\lambda(q_r(r_t))^{3/2}}$. From this set of equations we get

$$\tan \gamma \simeq i \frac{b + ia_2/\zeta}{1 - ia_1/\zeta} = ia \quad (69)$$

or

$$\begin{aligned} \zeta &= \lambda \int_{r_t}^{r_a} \sqrt{q} dr = \frac{1}{2i} \ln \frac{1-a}{1+a} + n\pi + \frac{5\pi}{12} \\ &= \arctan(ia) + \frac{5\pi}{12}, \end{aligned} \quad (70)$$

where $n = 0, 1, 2, \dots$ are the radial orders of the p -modes. This equation is a complex integral dispersion relation for the eigenfrequencies of nonradial p -modes. It is clear from this equation that the influence of the atmosphere on the p -modes is significant as $a \rightarrow 1$ for large $\lambda \gg 1$.

7. Eigenfrequencies of the radial oscillations

In this section we present the eigenvalues of the radial oscillations. The displacement in the atmosphere ($r \geq R_\odot$) may be expressed by Eq. (21) as

$$\xi_r \simeq -\frac{1}{r\sqrt{\rho}} \left[\left(\frac{g}{c^2 \omega^2} - \frac{1}{2H} \right) Y + \frac{dY}{dr} \right] e^{-i\omega t}. \quad (71)$$

Here r is not normalized. Substituting Eq. (55) into Eq. (71) and renormalizing the solution by replacing $C \Rightarrow -CR_\odot^2 h \sqrt{\rho_*}/\lambda$, where $\rho_* = \text{const}$, we have

$$\xi_r = Ch \left(\frac{\rho_*}{\rho} \right)^{1/2} q^{1/4} [\cos(\chi) - w \sin(\chi)] e^{-i\omega_1 t} e^{-\omega_2 t}, \quad (72)$$

$$U = -C \frac{h R_\odot \omega^2}{c^2 \lambda} \left(\frac{\rho_*}{\rho} \right)^{1/2} q^{-1/4} \sin(\chi) e^{-i\omega_1 t} e^{-\omega_2 t}, \quad (73)$$

$$p' = \rho g \xi_r - \rho c^2 U, \quad v_r = -i\omega \xi_r, \quad (74)$$

where $w(z) = \frac{1}{4\lambda} \frac{R_\odot}{h\sqrt{q}} \left(\frac{q'(z)}{q} + \frac{2h}{H} \right)$ and the normalized independent variables are connected at $r = 1 + \frac{h}{R_\odot} z$. The eigenfrequencies are determined from the equation $\chi(z = z_{\text{end}}) = n\pi$, where

$$\begin{aligned} \chi(z) &= \lambda \int_0^r \sqrt{q(r)} P(r) dr \\ &= \lambda \left(\int_0^1 \sqrt{q(r)} P(r) dr + \frac{h}{R_\odot} \int_0^z \sqrt{q(z)} P(z) dz \right). \end{aligned} \quad (75)$$

Table 1. The radial p -modes: $l = 0$

n	ν [μHz]	η	ω_2 [μHz]	n	ν [μHz]	η	ω_2 [μHz]
12	1839.9	0.994E-03	1.83	44	5990.6	0.893E-03	5.35
13	1970.6	0.993E-03	1.96	45	6117.6	0.888E-03	5.43
14	2098.6	0.992E-03	2.08	46	6244.5	0.882E-03	5.51
15	2229.1	0.991E-03	2.21	47	6370.7	0.876E-03	5.58
16	2356.5	0.989E-03	2.33	48	6509.4	0.883E-03	5.75
17	2489.2	0.988E-03	2.46	49	6626.2	0.880E-03	5.83
18	2639.1	0.987E-03	2.61	50	6755.5	0.878E-03	5.93
19	2759.7	0.986E-03	2.72	51	6884.0	0.875E-03	6.02
20	2896.5	0.985E-03	2.85	52	7013.3	0.872E-03	6.12
21	3033.8	0.984E-03	2.98	53	7209.8	0.868E-03	6.26
22	3171.6	0.982E-03	3.12	54	7342.2	0.865E-03	6.35
23	3308.3	0.980E-03	3.24	55	7473.8	0.862E-03	6.44
24	3443.7	0.978E-03	3.37	56	7606.3	0.859E-03	6.53
25	3572.6	0.975E-03	3.48	57	7737.9	0.856E-03	6.63
26	3701.4	0.973E-03	3.60	58	7869.9	0.853E-03	6.72
27	3829.6	0.970E-03	3.71	59	8002.0	0.850E-03	6.81
28	3956.1	0.967E-03	3.83	60	8135.5	0.848E-03	6.90
29	4083.8	0.964E-03	3.94	61	8267.6	0.845E-03	6.98
30	4211.8	0.961E-03	4.05	62	8401.2	0.842E-03	7.07
31	4335.3	0.956E-03	4.14	63	8533.2	0.839E-03	7.16
32	4460.8	0.954E-03	4.26	64	8666.8	0.836E-03	7.24
33	4589.0	0.952E-03	4.37	65	8798.8	0.833E-03	7.33
34	4718.0	0.949E-03	4.48	66	8932.4	0.829E-03	7.41
35	4847.3	0.946E-03	4.58	67	9064.5	0.826E-03	7.49
36	4975.8	0.942E-03	4.69	68	9096.5	0.826E-03	7.51
37	5105.9	0.936E-03	4.78	69	9227.0	0.823E-03	7.59
38	5232.8	0.929E-03	4.86	70	9359.0	0.819E-03	7.67
39	5359.0	0.924E-03	4.95	71	9491.0	0.816E-03	7.75
40	5485.2	0.919E-03	5.04	72	9621.5	0.813E-03	7.82
41	5610.5	0.913E-03	5.12	73	9753.5	0.810E-03	7.90
42	5736.7	0.904E-03	5.18	74	9884.0	0.806E-03	7.97
43	5863.7	0.899E-03	5.27	75	10016.0	0.803E-03	8.04

Here, z_{end} is the location of the upper turning point at CCTR, where $U(z_{\text{end}}) = 0$ is fulfilled.

The complex eigenfrequencies of radial oscillations are presented in Table 1. The frequency separations between adjacent modes ($\nu_{n+1} - \nu_n$) are generally around 128–132 μHz besides some bumps at 6–7 mHz. The latter could be due to a change in the structure of the atmospheric barrier at the position of the steepest gradient. Additional roots which would be a signature of chromospheric modes do not occur. The imaginary parts of the frequencies $\omega_2 = \text{Im}(\omega)$ grow with frequency ν . It is seen from Table 1 that additionally to radiative mechanisms the losses of wave energy by tunneling through the atmosphere are a significant mechanism for the formation of linewidths in the power spectrum of p -modes. After having analysed the case $l \neq 0$ in a future paper observed linewidths (Libbrecht 1988) will be compared to the theoretical predictions.

The relative discrepancies between the observations of Libbrecht et al. (1990) and our frequencies,

$$\delta\nu = (\nu_{\text{obs}} - \nu_{\text{th}}) / \nu_{\text{th}},$$

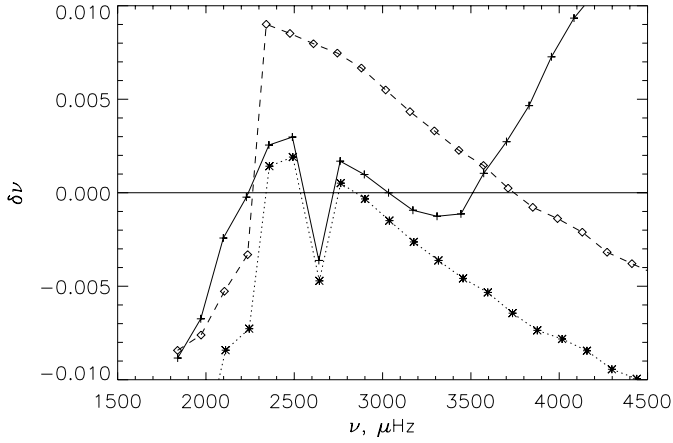


Fig. 6. Relative difference between the observed (ν_{obs}) and the calculated (ν_{th}) frequencies, $\delta\nu = (\nu_{\text{obs}} - \nu_{\text{th}})/\nu_{\text{th}}$, as a function of ν_{th} for radial p -modes. Marks on the curves identify the places of discrete frequencies. The dashed curve corresponds to the standard case: $\eta = 0$ (without tunneling) + old formula Eq. (13) + inner standard solar model up to $r = R_{\odot}$; the dotted curve corresponds to the same case as the dashed curve, but the upper part of the inner model was replaced by the lower part of the atmospheric model VAL3C to get a better fit of both models; the solid curve is the case where the influence of the whole atmosphere on the p -modes is taken into account.

are plotted in Fig. 6. All marks at the curves correspond to the discrete locations of the frequencies. First we have calculated frequencies by standard formula (13) (Christensen-Dalsgaard 1994) without including the atmospheric influence on the frequencies, using only the model of Stix (private communication) for the internal structure of the Sun. In this case both turning points are located inside the Sun ($r \leq R_{\odot}$) and the calculated frequencies are real. The results are shown by the dashed curve with squares. The second case is the dotted curve with stars where everything is similar to the first case, only the upper part of the model of Stix is replaced by the bottom part of the VAL3C model by fitting both models. It is seen that such a change of the model leads only to some parallel shift of $\delta\nu$, and the discrepancy problem remains. In the third case (continuous curve with crosses) we include the influence of the whole atmosphere, and the upper turning point is located in the CCTR.

It is seen that we get a strong decrease of the theoretical frequencies. This result is similar to that for our three layers isothermal model. After some oscillations around zero the function $\delta\nu$ becomes positive for the high-frequency p -modes. This curve is shown only up to ~ 4 mHz as we could not find a table of observed higher frequencies. However, the main result is the difference between the dashed (only the inner Sun) and the continuous (Sun with an atmosphere) curves and their dependence on ν . These results for the radial waves could be improved by abandoning the Cowling approximation, as the condition $\frac{\rho'}{\rho} \gg \frac{1}{g} \frac{d\Phi'}{dr}$ is violated close to the solar center.

An exact condition for the location of the upper turning point for the radial waves does not exist (contrary to the lower turning point for which the center of the Sun has been taken). For the nonradial waves these conditions are defined by Eqs. (33), (38).

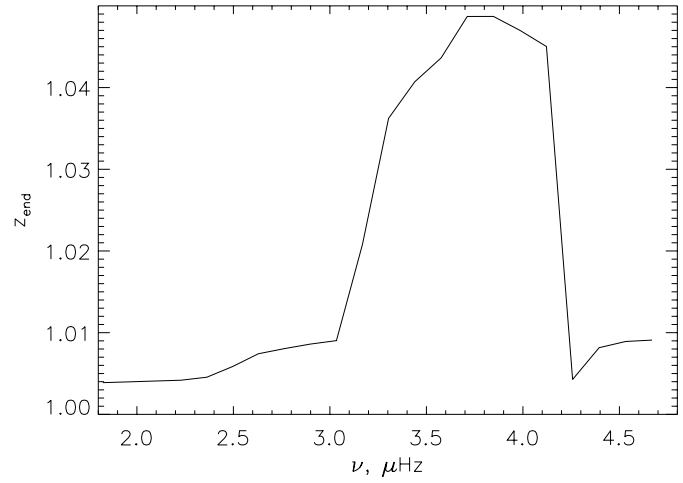


Fig. 7. Sensibility of frequencies to the location of the CCTR. At the plotted values of z_{end} the calculated frequencies coincide with the observed values: $\delta\nu = 0$. The results in Table 1 correspond to a fixed $z_{\text{end}} = 1.04$.

For radial waves we have chosen a turning point where CCTR has its sharpest temperature gradient, $z_{\text{end}} = 1.04$ (at a height of 1.04 h from the solar surface). In reality $z_{\text{end}} = z_{\text{end}}(\nu)$ must be considered. Further development of the theory is expected to answer this question. Now we can see from Fig. 7 how very small shifts in z_{end} may influence the frequencies. The figure shows the location of the upper turning point for the observed oscillations. It means that for these values of z_{end} in the curve the discrepancy function is zero, $\delta\nu = 0$.

Now we can easily find the average flux of energy transmitted through the upper boundary, as all eigenfunctions are known:

$$\overline{F_r} = C^2 \omega_2 g h^2 \rho_* \sqrt{|q|} \cos^2 \left(\frac{1}{4} \varphi_q + \arctan \eta \right), \quad (76)$$

where φ_q is an argument of $q(z_{\text{end}})$: $q = |q| \exp(i\varphi_q)$. It is clear that the transport of energy across the boundary is connected to upward propagating, tunneling waves with $\omega_2 \neq 0$. This becomes clear if we introduce the eigenfunction of the form

$$\xi_r \approx -Ch \left(\frac{\rho_*}{\rho} \right)^{1/2} q^{1/4} i \times (e^{-\chi_2} \sin \chi_1 + i e^{i\chi_1} \cosh \chi_2) e^{-i\omega t}, \quad (77)$$

where $\chi = \chi_1 - i\chi_2$ has been used. In this equation the first term corresponds to standing waves for which the locations of nodes are determined by $\chi_1 = n\pi$, they do not depend on time. The second term corresponds to the propagating, tunneling waves. Using Eq. (76) we can estimate the energy flux which p -modes lose due to tunneling, as the observed amplitudes at the photospheric levels are known. Numbers will be given in a future paper with calculations for non-radial waves.

8. Discussion

In the present paper we developed an asymptotic theory which is too rough for calculating precise frequencies and comparing

them with observations. In highly structured regions of the atmosphere with characteristic scales $\lesssim \lambda$ (λ is the wavelength) the accuracy of our asymptotic eigenfunctions gets worse. In such regions the subsequent terms in the series expansions of the solutions could in principle be taken into account. However, the contributions of these narrow regions to the integrals in the eigenvalue calculation are insignificant. Nevertheless, we can infer answers to the following questions: how are the frequencies of the p -modes shifted by the tunneling of the waves, how should the upper boundary conditions be taken into account in more exact numerical calculations of frequencies, how these frequencies depend on the location of CCTR, and how the peaks at high frequencies become eigenfrequencies of the Sun such as the low-frequency p -modes?

Now we will shortly discuss the approximations used in the present work. The first approximation is that of adiabaticity. Dzhililov & Babaev (1995) and Babaev & Dzhililov (1996) have investigated analytically the interaction of acoustic waves with radiation for the Eddington approximation. It was shown that coupling of acoustic and radiative (thermal) waves occurs in a narrow region of the photosphere where the free paths of photons are comparable to the wavelengths of the acoustic waves. At higher chromospheric levels the phase velocities of these waves are strongly different and acoustic waves become adiabatic again. This means the contribution of the radiative losses is mainly affecting the decay rate η of the p -modes but not ν . Hence the amplitude decay of p -modes due to radiative losses and due to tunneling losses should explain the linewidths in the power spectrum.

Then, the Cowling approximation is used. Pekeris (1938) and Tassoul (1990) considered the full system with Eulerian perturbations of the gravity potential $\Phi' \neq 0$. We get a situation similar to that with radiation. The coupling of acoustic waves with gravity perturbations is considerable only at photospheric levels. In the upper layers of the atmosphere the behavior of the gravity perturbations becomes exponential.

For the solution of the boundary value problem we have used a free surface condition, $\text{div} \cdot \vec{v} = 0$, at the upper boundary (CCTR). This condition followed from the fact that waves with a complex radial wavenumber (in physics such waves are called inhomogeneous waves) may exist in a limited volume only. In our case this means that we cannot use a radiation condition for acoustic waves propagating upward into the semi-infinite corona. With increasing $r \rightarrow \infty$ the amplitude of linear waves increases. Then it was shown that the flux of energy transported by waves tunneling through the upper boundary is not zero. If the waves cannot run upward into the infinite corona in the linear regime, the question arises what should be done with this flux of energy. Two ways could perhaps solve this problem. If the amplitude of the waves in the upper chromosphere and in CCTR is large, then a nonlinear mechanism of dissipation must be included. In the opposite case (small amplitude) the generation of surface gravity oscillations by the p -modes should be considered.

So let us focus on the linear approximation which is important for the high levels of the chromosphere and for the CCTR.

As the amplitudes of the fluid velocity ($v_0 \sim 10 \text{ cm s}^{-1}$) of the p -modes are known at the photospheric level we can use our eigenfunctions (Eq. (72)) and estimate the amplitudes at any level of the atmosphere. If we suppose that the observed amplitude is $|v_{\text{max}}|_{\text{phot}} \simeq v_0$ then we can define the constant C for the amplitude, and as a result we have

$$|v_r|_{\text{max}} \approx v_0 \left(\frac{\rho_*}{\rho} \right)^{1/2} \left| \frac{q}{q_*} \right|^{1/4}.$$

If the power spectrum of the 5-min oscillations is detected in the evanescent zone (Fig. 2) with the parameters $z \simeq -0.05$, $\rho_* \approx 0.3 \times 10^{-6} \text{ g cm}^{-3}$, $\omega_c^2 \sim 10^{-3} \text{ s}^{-2}$, $q_* \simeq -1$, then we have in the upper chromosphere $z \simeq 0.8$, $\rho \approx 0.3 \times 10^{-12} \text{ g cm}^{-3}$, $\omega_c^2 \sim 10^{-6} \text{ s}^{-2}$, $q \simeq 1$, and $|v_r|_{\text{max}} \approx 0.1 \text{ km s}^{-1} \ll v_{\text{phase}} \simeq c \simeq 10 \text{ km s}^{-1}$. It means that the linear approximation is justified.

The linear condition $|\partial v_r / \partial t| \gg |(v \cdot \nabla) v_r|$ can be rewritten as $|\partial \xi_r / \partial r| \ll 1$. At CCTR $\partial \xi_r / \partial r \sim \sin(\chi) \rightarrow 0$, as the dispersion relation $\chi = n\pi$ is obeyed. So, in the whole domain of integration up to the CCTR we have linear oscillations with only a slight deformation of the wave profile.

In this way there arises the possibility of a conversion of the p -modes into surface gravity oscillations. Unlike the free surface gravity oscillation (f -modes) the forced oscillations are compressible, $\text{div} \cdot \vec{v} \neq 0$ (but close to zero) and for the forced f -modes $\omega^2 \neq gk_{\perp}$. The penetration depth of these waves from CCTR downward toward the photosphere depends on the p -mode frequencies. The generation of forced f -modes by p -modes has a resonant character. This means, that the amplitudes of these oscillations increase in time as $\sim t$. Hence we have a reasonable heating mechanism by p -modes in the quiet CCTR.

So we have a rather complicated wave structure in the upper atmosphere: on the standing p -modes upgoing tunneling waves and weak downgoing forced f -modes are imposed. Observations gave an evidence for such a pattern (for the $(V - V)$ and $(I - I)$ phase spectra see, e.g., Fleck & Deubner (1989) and Muglach & Fleck (1999)) and for $\omega^2 \neq gk_{\perp}$ for the f -modes (Antia & Basu 1999) in the whole upper atmosphere.

The eigenfrequency resulting from our present work are incomplete, as the generation of forced gravity oscillations by the p -modes in CCTR must be included. This will be the topic of a future paper. Of course, our theoretical conclusion about the behavior of the upper transition region between the corona and chromosphere as a free surface needs support by observations. For this purpose it is sufficient to show that in the wave motions of the CCTR the Lagrangian density perturbations $\delta\rho$ are close to zero.

In the final figure we have shown that the eigenfrequencies of the p -modes are very sensitive to the location of the upper CCTR boundary. Hence a small shift of CCTR by solar activity should already lead to some variations of the frequencies of oscillations obtained from the quiet Sun compared to those from periods with higher solar activity.

Acknowledgements. Michael Stix kindly provided detailed tables from his internal solar model calculations and reviewed the present paper. The critical comments and suggestions by Kris Murawski and

by Michael Stix helped to improve an earlier version of the paper. The authors gratefully acknowledge financial support of the present work by the German Space Research Center (DLR) under grant No. 50 QL 9601 9, by the German Science Foundation (DFG) under grant No. 436 RUS 113/81/3, and by the Russian Foundation for Basic Research (RFBR) under grant No. 98-02-17062.

Appendix A: asymptotic solution around the upper turning point

This is a rather technical and longish section which is available in electronic form by using anonymous ftp from aipsoe.aip.de (141.33.64.1): change to directory /pub/p-modes and get the file Append.ps.

References

- Abramowitz M., Stegun I.A., 1984, Pocketbook of Mathematical Functions. Verlag Harri Deutsch, Thun – Frankfurt/Main
- Al N., Bendlin C., Kneer F., 1998, A&A 336, 743
- Ando H., Osaki Y., 1977, PASJ 29, 221
- Antia H.M., Basu S., 1999, ApJ 519, 400
- Antia H.M., Chitre S.M., 1998, A&A 339, 239
- Babaev E.S., Dzhililov N.S., 1996, Astron. Letters 22, 3
- Balmforth N., Gough D.O., 1990, ApJ 362, 256
- Basu S., Christensen-Dalsgaard J., Schou J., Thompson M.J., Tomczyk S., 1996, ApJ 460, 1064
- Baudin F., Bocchialini K., Koutchmy S., 1996, A&A 314, L9
- Böhmer S., Rüdiger G., 1999, A&A 351, 747
- Christensen-Dalsgaard J., 1994, Stellar Oscillations. Institut for Fysik og Astronomi, Aarhus Universitet
- Christensen-Dalsgaard J., Thompson M.J., 1997, MNRAS 284, 527
- Deubner F.L., Fleck B., 1989, A&A 213, 423
- Deubner F.L., Fleck B., 1990, A&A 228, 506
- Doyle J.G., Van Den Oord C.H.J., O’Shea E., Banerjee D., 1998, Solar Phys. 181, 51
- Duvall T.L., Harvey J.W., Jefferis S.M., Pomerantz M.A., 1991, ApJ 373, 308
- Dzhililov N.S., Babaev E.S., 1995, Astron. Letters 21, 54
- Dzhililov N.S., Staude J., 1995, A&A. 303, 561
- Elsworth Y., Howe R., Isaak G., et al., 1993, In: Brown T.N. (ed.) GONG 1992: Seismic Investigation of the Sun and Stars. ASP Conf. Series 142, p. 107
- Evans D.J., Roberts B., 1990, ApJ 356, 704
- Federuk M.V., 1983, Asymptotic methods for ordinary differential equations. Moscow, Nauka
- Fernandes D.N., Scherrer P.H., Tarbell T.D., Title A.M. 1992, ApJ 392, 736
- Fleck B., Deubner F.L., 1989, A&A 224, 245
- Fleck B., Deubner F.L., 1990, A&A 228, 506
- Gabriel M., 1992, A&A 265, 771
- Gabriel M., 2000, A&A 353, 399
- Garcia R.A., Palle P.L., Turk-Chieze S., et al., 1998, ApJ 504, L51
- Gough D.O., 1986, In: Osaki Y. (ed.) Hydrodynamic and Magnetohydrodynamic Problems in the Sun and Stars. Univ. Tokio Press, p. 117
- Gouttebroze P., Vial J.C., Bocchialini K., Lemaire P., Leibacher J.W., 1999, Solar Phys. 184, 253
- Hindman B.W., Zweibel E.G., 1994, ApJ 436, 929
- Keldish M., 1951, Reports of Acad. Sci. USSR 87, 11
- Kneer F., von Uexkull M., 1993, A&A 274, 584
- Kumar P., Lu E., 1991, ApJ 375, L35
- Lamb H., 1908, Proc. Roy. Soc. Lond. 7, 122
- Lamb H., 1932, Hydrodynamics. 6th ed., Cambridge Univ. Press
- Langer R.E., 1930, Trans. Amer. Math. Soc. 32, 238
- Libbrecht K.G., 1988, ApJ 334, 510
- Libbrecht K.G., Woodard M.F., Kaufman J.M., 1990, ApJS 74, 1129
- McKenzie J.F., 1971, A&A 15, 450
- Medrek M., Murawski K., 2000, ApJ 529, 548
- Milford P.N., Scherrer P.H., Frank Z., Kosovichev A.G., Gough D.O., 1993, In: Gong 1992: Seismic Investigation of the Sun and Stars. ASP Conf. Series Vol. 42, p. 97
- Morel P., Provost J., Berthomieu G., 1997, A&A 327, 349
- Muglach K., Fleck B., 1999, Proc. 8th SOHO Workshop, ESA SP-446, 499
- Murawski K., 2000 a, A&A 358, 343
- Murawski K., 2000 b, ApJ 537, 495
- Obridko, V.N., Staude J., 1988, A&A 189, 232
- Pekeris C.L., 1938, ApJ 88, 189
- Rosenthal C.S., Christensen-Dalsgaard J., Nordlund Å., Stein R.F., Trampedach R., 1999, A&A 351, 689
- Roxburgh I.W., Vorontsov S.V., 1994, MNRAS 267, 297
- Staiger J., 1987, A&A 175, 263
- Staude J., 1985, Astron. Nachr. 306, 197
- Steffens S., Deubner F.L., 1999, In: High Resolution in Solar Physics: Theory, Observations, and Techniques. ASP Conf. Ser. Vol. 183, p. 426
- Steffens S., Schmitz F., 2000, A&A 354, 280
- Stix M., 1989, The Sun. Springer, Berlin
- Stix M., Skaley, D., 1990, A&A 232, 234
- Tamarkin J., 1928, Math. Zeitschrift 27, 1
- Tassoul M., 1980, ApJS 43, 469
- Tassoul M., 1990, ApJ 358, 313
- Ulrich R.K., Rhodes E.J., 1977, ApJ 218, 521
- Unno W., Osaki Y., Ando H., Saio H., Shibahashi H., 1989, Nonradial Oscillations of Stars. University of Tokio Press
- Vandakurov Y.V., 1967, AZh 44, 786
- Vernazza J.E., Avrett E.H., Loeser R., 1981, ApJS 45, 635
- Von Uexküll M., Kneer F., 1995, A&A 294, 252
- Willems B., Van Hoolst T., Smeyres P., 1997, A&A 326, 1055